A novel mechanism for the establishment of sister chromatid cohesion by the *ECO1* acetyltransferase

Vincent Guacci[a], Jeremiah Stricklin[a], Michelle S. Bloom[a], Xuánzōng Guō[b], Meghna Bhatter[a], and Douglas Koshland[a]

[a]Department of Molecular and Cell Biology, University of California, Berkeley, Berkeley, CA 94720; [b]Department of Biology, Massachusetts Institute of Technology, Cambridge, MA 02139

ABSTRACT **Cohesin complex mediates cohesion between sister chromatids, which promotes high-fidelity chromosome segregation. Eco1p acetylates the cohesin subunit Smc3p during S phase to establish cohesion. The current model posits that this Eco1p-mediated acetylation promotes establishment by abrogating the ability of Wpl1p to destabilize cohesin binding to chromosomes. Here we present data from budding yeast that is incompatible with this Wpl1p-centric model. Two independent in vivo assays show that a *wpl1*Δ fails to suppress cohesion defects of *eco1*Δ cells. Moreover, a *wpl1*Δ also fails to suppress cohesion defects engendered by blocking just the essential Eco1p acetylation sites on Smc3p (K112, K113). Thus removing *WPL1* inhibition is insufficient for generating cohesion without *ECO1* activity. To elucidate how *ECO1* promotes cohesion, we conducted a genetic screen and identified a cohesion activator mutation in the *SMC3* head domain (D1189H). *Smc3-D1189H* partially restores cohesion in *eco1*Δ *wpl1*Δ or *eco1* mutant cells but robustly restores cohesion in cells blocked for Smc3p K112 K113 acetylation. These data support two important conclusions. First, acetylation of the K112 K113 region by Eco1p promotes cohesion establishment by altering Smc3p head function independent of its ability to antagonize Wpl1p. Second, Eco1p targets other than Smc3p K112 K113 are necessary for efficient establishment.**

Monitoring Editor
Kerry S. Bloom
University of North Carolina

Received: Aug 8, 2014
Revised: Oct 6, 2014
Accepted: Oct 27, 2014

INTRODUCTION

Cohesin is an essential, evolutionarily conserved four-subunit complex that tethers sister chromatids from their formation in S phase through metaphase (Guacci *et al.*, 1997; Michaelis *et al.*, 1997; Losada *et al.*, 1998; Sumara *et al.*, 2000; Tomonaga *et al.*, 2000). This tethering (cohesion) enables each sister chromatid pair to achieve a bipolar attachment to the mitotic spindle and thereby promotes high-fidelity chromosome segregation at anaphase. In budding yeast, the cohesin subunits are named *MCD1/SCC1*, *SMC1*, *SMC3*, and *SCC3/IRR1* (Figure 1A; Guacci *et al.*, 1997; Michaelis *et al.*, 1997). Cohesin also plays roles in chromosome condensation, transcriptional regulation, and DNA damage repair (Guacci *et al.*, 1997; Rollins *et al.*, 2004; Ström *et al.*, 2004; Unal *et al.*, 2004). These processes are temporally and spatially distinct. For example, cohesion is established during S phase, whereas condensation occurs during mitosis (Onn *et al.*, 2008). Cohesin binds specific sites called cohesin-associated regions (CARs) for cohesion and condensation, whereas it binds any DNA adjacent to double-strand breaks to help facilitate damage repair (Blat and Kleckner, 1999; Megee *et al.*, 1999; Laloraya *et al.*, 2000; Kim *et al.*, 2002; Ström *et al.*, 2004; Unal *et al.*, 2004). Elucidating the mechanisms underlying the temporal and spatial regulation of cohesin is crucial to understanding how cohesin performs its diverse functions and how it tethers chromatin.

A simple model for the regulation of cohesion establishment was built around the cohesin inhibitor, termed *WPL1/RAD61* in yeast (Rowland *et al.*, 2009; Sutani *et al.*, 2009; Chan *et al.*, 2012). This *WPL1*-centric model emerged from three observations in budding yeast. First, the *ECO1/CTF7* protein (Eco1p/Ctf7p) acetylates the Smc3p cohesin subunit at lysine residues 112 and 113 (K112, K113),

This article was published online ahead of print in MBoC in Press (http://www.molbiolcell.org/cgi/doi/10.1091/mbc.E14-08-1268) on November 5, 2014.

Address correspondence to: Vincent Guacci (guacci@berkeley.edu).

Abbreviations used: BEN, benomyl; CPT, camptothecin.

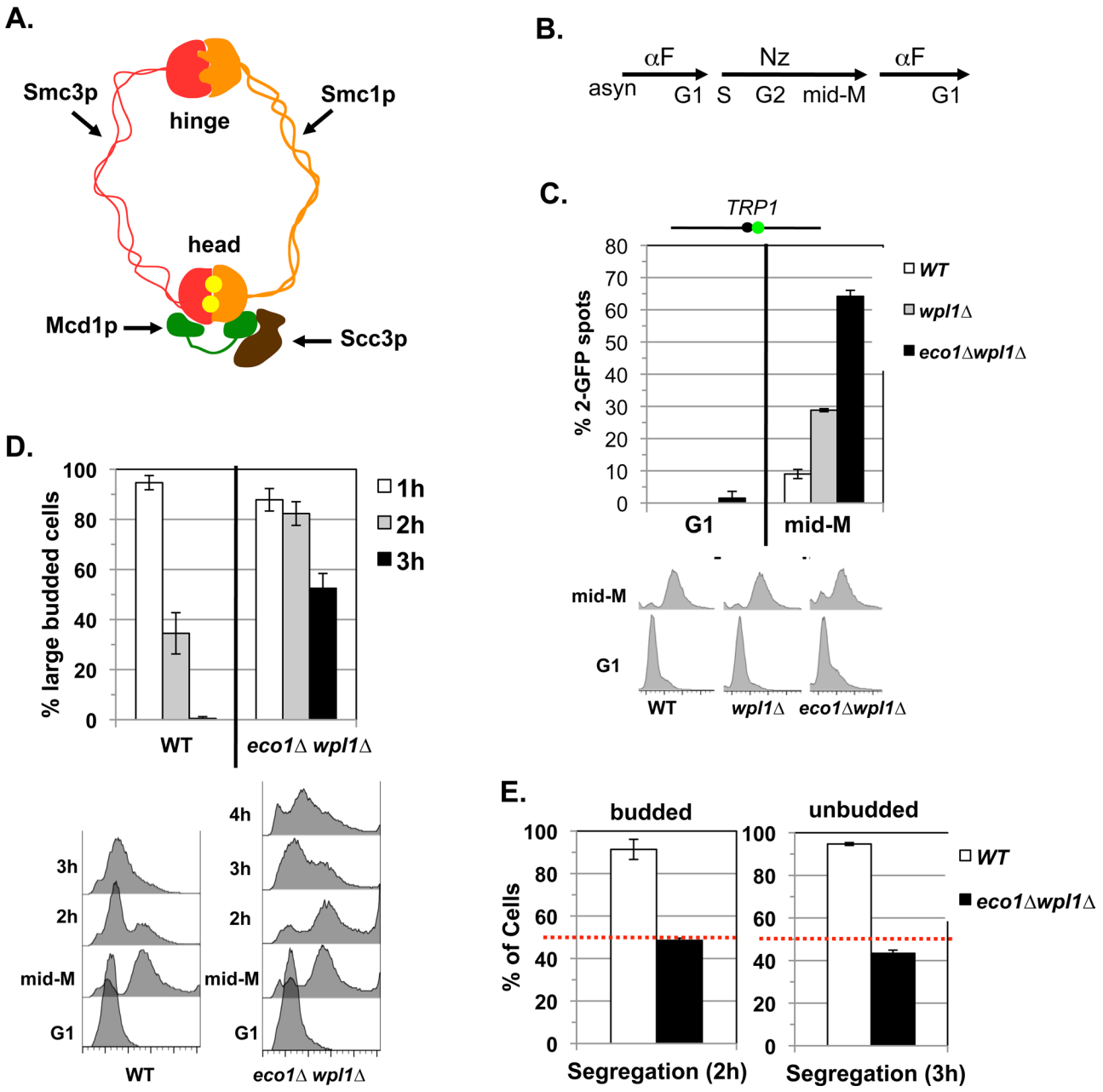

FIGURE 1: *eco1Δ wpl1Δ* cells lack segregation-competent cohesion. (A) Cartoon depicting the structure of the cohesin complex. Smc3p (red) interacts with Smc1p (orange) at the hinge and head domains. Mcd1p (green) binds to both the Smc1p and Smc3p heads. Scc3p (brown) binds to Mcd1p. Two Walker A/B ATPases (yellow balls) are in the heads. (B) Regimen used to assess segregation-competent segregation in cells. (C) Cohesion loss at *CEN*-proximal *TRP1* locus at mid–M phase arrest. Haploid WT (VG3460-2A), *eco1Δ wpl1Δ* (VG3502-1C), and *wpl1Δ* (VG3513-1B) strains were arrested in G1 using αFactor at 23°C and then released and rearrested in mid–M phase at 23°C using nocodazole (*Materials and Methods*). The percentage of cells with two GFP spots (separated sister chromatids) is plotted (top) along with DNA content (bottom). The lack of G1 cells with two GFP spots demonstrates absence of preexisting aneuploidy. The green dot above the graph shows the position of LacO arrays relative to the centromere. (D, E) Assay for segregation-competent cohesion. Haploid WT (VG3460-2A) and *eco1Δ wpl1Δ* (VG3502-1C) cells were treated as in B. (D) Assessment of cell-cycle progression after release from mid–M (nocodazole) arrest. Percentage of large-budded cells remaining at 1, 2, and 3 h after release from mid–M phase arrest (top) and DNA content (bottom). (E) Segregation of chromosome IV sister chromatids after release from mid–M phase. Proper segregation in large-budded cells 2 h after release (left). Proper segregation in unbudded cells 3 h after release (right). Random segregation is 50% and is marked by a dotted red line. Data for C–E are from two independent experiments; 100–300 cells scored for each data point.

and this K113 acetylation is required to allow chromatin-bound cohesin to establish cohesion (Skibbens *et al.*, 1999; Tóth *et al.*, 1999; Rolef Ben-Shahar *et al.*, 2008; Unal *et al.*, 2008; Zhang *et al.*, 2008). Second, deleting *WPL1* (*wpl1Δ*) suppresses the inviability of cells deleted for *ECO1* (*eco1Δ*) or bearing the *SMC3* acetylation-null *smc3-K113R* or *smc3-K112R,K113R* allele (lysine to arginine; Rolef Ben-Shahar *et al.*, 2008; Rowland *et al.*, 2009; Sutani *et al.*, 2009). Third, the stability of cohesin binding to chromosomes is decreased

in *eco1* mutants relative to wild type but is more stable than wild type in either *wpl1*Δ or *eco1*Δ *wpl1*Δ cells (Chan *et al.*, 2012). Based on these and other studies, it was proposed that a ring-like cohesin molecule topologically entraps both sister chromatids to generate cohesion (Onn *et al.*, 2008; Chan *et al.*, 2012). In this scenario, Wpl1p inhibits cohesion establishment by destabilizing cohesin binding (Supplemental Figure S1). Acetylation of Smc3p at K112, K113 promotes cohesion by antagonizing Wpl1p, thereby stabilizing cohesin binding/sister entrapment.

Recent data contradict the Wpl1p-centric view of cohesion regulation. Previously we and two other laboratories showed that although viable, *eco1*Δ *wpl1*Δ mutants have defects in cohesion as severe as that of *eco1* mutants (Rowland *et al.*, 2009; Sutani *et al.*, 2009; Guacci and Koshland, 2012). We extended this result by showing that *eco1*Δ *wpl1*Δ cells are defective in the establishment of cohesion (Guacci and Koshland, 2012). These results led us to three conclusions (Guacci and Koshland, 2012). First, since budding yeast can be viable with very little, if any, sister chromatid cohesion, a second mechanism for bipolar attachment of sister chromatids to the spindle must exist. We provided evidence that this alternative mechanism in yeast results from the unusual precocious assembly of the spindle and attachment of microtubules to kinetochores on partially replicated chromosomes during S phase. Second, *wpl1*Δ must restore viability to *eco1*Δ cells by promoting an essential cohesin function distinct from sister chromatid cohesion. Several reports provide evidence that this function is condensation, as Wpl1p inhibits cohesin-dependent chromosome condensation in yeast (Guacci and Koshland, 2012; Lopez-Serra *et al.*, 2013; Eng *et al.*, 2014). Third, Eco1p must promote cohesion establishment independent of any need to antagonize Wpl1p inhibition. However, evidence showing that Eco1p mediates Wpl1p-independent generation of cohesion was lacking.

Our conclusions have been challenged by a disagreement in the field about the magnitude and the nature of the cohesion defect in the *eco1*Δ *wpl1*Δ cells. All groups used the gold standard in the field to assess cohesion—direct in vivo monitoring of discrete chromosome loci marked with green fluorescent protein (GFP). Three groups observed a 60–70% cohesion defect in *eco1*Δ *wpl1*Δ cells, which is as severe as seen in cohesin complex mutants (Rowland *et al.*, 2009; Sutani *et al.*, 2009; Guacci and Koshland, 2012). Two of these groups postulated that cohesion might still exist on chromosomes at some sites distinct from loci tagged by GFP (Rowland *et al.*, 2009; Sutani *et al.*, 2009). One group noted that a minor portion of minichromosomes isolated from *eco1*Δ *wpl1*Δ cells showed altered gel mobility compared with *eco1* mutants, which they interpreted as evidence of cohesion (Rowland *et al.*, 2009). If true, such residual cohesion could enable bipolar chromosome attachments and thereby promote segregation and viability. Although there is value in resolving this issue, it would not alter the fact that cohesion establishment is severely disrupted at multiple loci in *eco1*Δ *wpl1*Δ cells. Finally, one group observed only a 20% cohesion defect in *eco1*Δ *wpl1*Δ cells despite using the same genetic background as two groups observing the 60–70% defect (Rolef Ben-Shahar *et al.*, 2008). This discrepancy might reflect secondary mutations arising during the outgrowth of *eco1*Δ *wpl1*Δ mutants. Any interpretation of cohesion in *eco1*Δ *wpl1*Δ cells is further complicated by the fact that Wpl1p plays a positive as well as an inhibitory role in cohesion. This positive role is revealed in budding yeast by a partial defect in cohesion establishment and reduced cohesin binding to chromosomes in *wpl1*Δ cells (Rowland *et al.*, 2009; Sutani *et al.*, 2009; Guacci and Koshland, 2012).

Here we provide in vivo evidence that *eco1*Δ *wpl1*Δ cells lack sufficient cohesion to promote chromosome segregation. We also conducted a genetic screen to identity mutations that restore cohesion in *eco1*Δ *wpl1*Δ cells. One such cohesion activator mutation in the Smc3p head domain changes the highly conserved aspartic acid residue 1189 to histidine (*smc3-D1189H*) and partially restores cohesion to *eco1*Δ *wpl1*Δ cells. The *D1189H* mutation restores nearly wild-type levels of cohesion to *smc3-K112R,K113R* cells when assayed in-*cis* (i.e., chimeric *smc3-RR-D1189H* allele). In contrast, a *wpl1*Δ has no effect on the major cohesion defect engendered by *smc3-K112R,K113R*. Our results provide strong evidence that Eco1p acetylation of Smc3p modulates its head domain to promote cohesion establishment. This modulation is independent of any antagonism of Wpl1p and occurs at a step distinct from cohesin binding to chromosomes. Our data also suggest that Eco1p has additional targets that promote efficient cohesion establishment other than the Smc3p K112, K113 residues that have been the prime focus of establishment studies.

RESULTS

*eco1*Δ *wpl1*Δ cells have little or no functional cohesion

Several groups, including ours, found major cohesion defects in *eco1*Δ *wpl1*Δ cells when directly monitoring cohesion at specific chromosomal loci, but one group reported significantly less of a defect (Rowland *et al.*, 2009; Sutani *et al.*, 2009; Guacci and Koshland, 2012; Rolef Ben-Shahar *et al.*, 2008). To rule out the possibility that secondary mutations arose during outgrowth of our strains to generate the dramatic cohesion defect, we used a conditional *eco1*Δ *wpl1*Δ strain. For this purpose, we constructed a conditional *ECO1* allele using the auxin-inducible degron system (AID), which entailed C-terminal addition of *3V5* and *AID2,* termed *ECO1-AID* (*Materials and Methods*; Eng *et al.*, 2014). We then deleted *WPL1* in the *ECO1-AID* background (*ECO1-AID wpl1*Δ) and compared its phenotypes to wild-type, *ECO1-AID* alone, and *eco1*Δ *wpl1*Δ strains. Addition of auxin to media induces degradation of the essential Eco1-AIDp so the *ECO1-AID* strain becomes inviable (Supplemental Figure S2A). A *wpl1*Δ suppresses the auxin-dependent inviability of the *ECO1-AID* allele, recapitulating the ability of *wpl1*Δ to bypass an essential function of Eco1p (Supplemental Figure S2A). Moreover, the *ECO1-AID wpl1*Δ strain also exhibits an auxin-dependent benomyl sensitivity similar to that of *eco1*Δ *wpl1*Δ cells, consistent with a cohesion defect.

We next asked whether a severe cohesion defect is indeed generated in the first cell cycle after Eco1p depletion in a *wpl1*Δ background. After strains were arrested in G1, auxin was added to deplete Eco1-AIDp. Cells were released from G1 into media containing auxin and nocodazole to arrest them in mid–M phase under conditions in which Eco1-AIDp is depleted over this entire cell-cycle interval (Supplemental Figure S2B). Yeast cells are termed mid–M phase because sister chromatids have cohesion and are condensed (Guacci *et al.*, 1994). Cohesion was scored at a *CEN*-distal (*LYS4*) locus. In this assay, a failure to establish or maintain cohesion leads to the presence of two GFP foci (spots) in cells. Wild-type cells have robust cohesion, as shown by few mid–M phase cells with two GFP spots, whereas *ECO1-AID* cells have a severe defect, as shown by the high percentage of cells with two GFP spots (Supplemental Figure S2C, left). Of importance, >70% of either *ECO1-AID wpl1*Δ or *eco1*Δ *wpl1*Δ cells have two GFP spots, indicating a cohesion defect as severe as seen in *ECO1-AID* cells (Supplemental Figure S2C, right). Few G1 cells from any strain had two GFP spots, demonstrating the absence of preexisting aneuploidy, which indicates that mid–M phase cells with two GFP spots arose due to defective cohesion.

Thus the first cell-cycle depletion of Eco1p in the *wpl1*Δ background recapitulates studies in which *eco1*Δ *wpl1*Δ cells had both major cohesion defects and benomyl sensitivity (Sutani *et al.*, 2009; Guacci and Koshland, 2012). This result makes it highly unlikely that secondary mutations are responsible for these *eco1*Δ *wpl1*Δ mutant phenotypes.

Observing major cohesion defects at specific loci in *eco1*Δ *wpl1*Δ cells does not rule out the possibility that cohesion exists at other chromosomal regions. If such residual cohesion exists, it should enable bipolar chromosome attachments and thereby promote sister segregation and viability. We assessed this possibility using a nocodazole-arrest release segregation assay (Figure 1B and *Materials and Methods*). Arrest in mid–M phase using nocodazole abrogates any early S-phase attachments that enable cohesion-independent segregation (Guacci and Koshland, 2012). Subsequent release from nocodazole arrest allows spindles to form, kinetochores to attach to microtubules, and cells to complete mitosis. We labeled the *CEN4*-proximal (*TRP1*) locus because chromosome IV is the second largest yeast chromosome. As such, it is an excellent substrate to assess whether cohesion exists at other loci along a chromosome and thereby enable bipolar attachment in mitosis to promote subsequent segregation (i.e., segregation-competent cohesion).

To assess segregation-competent cohesion, wild-type and *eco1*Δ*wpl1*Δ strains were released from G1 into media containing nocodazole to induce arrest in mid–M phase as large-budded cells lacking spindles. Consistent with our previous analyses, cohesion was robust in wild-type cells and severely defective in *eco1*Δ *wpl1*Δ cells (Figure 1C). Mid–M phase–arrested cells were allowed to complete mitosis and arrest in G1 by removing nocodazole and adding α-factor (Figure 1B). We first monitored cell-cycle progression. By 2 h after release from nocodazole arrest, many wild-type cells completed anaphase and exited mitosis, as seen by a decrease in the percentage of large-budded cells and the appearance of cells with 1C DNA content (Figure 1D). In contrast, most *eco1*Δ *wpl1*Δ cells remained large budded and had 2C DNA content. By 3 h, virtually all wild-type cells had completed mitosis and arrested in G1, whereas only ~50% of *eco1*Δ *wpl1*Δ cells had done so. This mitotic progression delay of *eco1*Δ *wpl1*Δ cells is characteristic of checkpoint-mediated delays after global cohesion abrogation via mutants in *ECO1* or cohesin subunits (Skibbens *et al.*, 1999; Stead *et al.*, 2003; Noble *et al.*, 2006).

We then scored chromosome IV segregation in large-budded cells 2 h after release from nocodazole arrest (*Materials and Methods*). More than 80% of large budded wild-type cells had one GFP spot in each daughter nucleus, indicating segregation of sister chromatids (Figure 1E, left). In contrast, only 50% of large-budded *eco1*Δ *wpl1*Δ cells showed segregation to the daughter nuclei. We also scored segregation in unbudded cells, which have completed mitosis and rearrested in G1 (*Materials and Methods*). Approximately 90% of unbudded wild-type cells exhibit proper chromosome IV segregation, whereas only ~50% of unbudded *eco1*Δ *wpl1*Δ cells showed segregation (Figure 1E, right). Moreover, sub-1C and >1C peaks are observed in *eco1*Δ *wpl1*Δ cells at 4 h after release, consistent with a global defect in segregation (Figure 1D). Random segregation (50%) is expected if there is a complete lack of cohesion, leading us to conclude that *eco1*Δ *wpl1*Δ cells have little or no segregation-competent cohesion.

A genetic screen identified *smc3-D1189H* as a mutation that partially restores cohesion in *eco1*Δ *wpl1*Δ *cells*

Our previous study indicated that cohesin mutants use an alternative mechanism to segregate their sister chromatids despite abrogation of cohesion (Guacci and Koshland, 2012). This cohesion-independent mechanism depends on the persistence of bipolar sister chromatid attachments to kinetochore microtubules generated in early S phase (Figure 2A). Our finding that *eco1*Δ *wpl1*Δ cells have little or no segregation-competent cohesion suggests that they also depend on this alternative pathway. This view is consistent with the observation that *eco1*Δ *wpl1*Δ cells are inviable when exposed to low levels of the microtubule-depolymerizing drug benomyl (Figure 2A; Sutani *et al.*, 2009; Guacci and Koshland, 2012). These cells are also very sensitive to camptothecin, a topoisomerase I inhibitor that induces DNA damage, possibly because without cohesion, they are less competent to repair DNA damage (Guacci and Koshland, 2012). We reasoned that screening for *eco1*Δ *wpl1*Δ cells resistant to either drug should select for suppressor mutations that restore cohesion establishment in the absence of both Eco1p and Wpl1p (see Supplemental Figure S3 and *Materials and Methods* for screen details).

Only about 1 in 1 million *eco1*Δ *wpl1*Δ cells exhibited benomyl or camptothecin resistance. Suppressors were then tested for resistance to the other drug (i.e., benomyl-resistant clones were assayed for camptothecin resistance). Only a small number of clones exhibited dual drug resistance, suggesting that suppressing the cohesion defect of *eco1*Δ *wpl1*Δ cells required specific and rare changes in genes. All clones exhibiting dual drug resistance were subjected to whole-genome sequencing. The same amino acid change in Smc3p was found in four independent clones exhibiting dual drug resistance. This mutation is located in the Smc3p head domain and changed aspartic acid residue 1189 to histidine (D1189H; Figure 2B). To assess linkage between the *smc3-D1189H* mutation and the drug resistance, we reintroduced this allele in place of *SMC3* in the parent *eco1*Δ *wpl1*Δ (*Materials and Methods*). We compared one of the screen-derived *D1189H* suppressors (sup #1) to the rebuilt *smc3-D1189H eco1*Δ *wpl1*Δ strain and found that they are phenotypically indistinguishable (Figure 2C). This result confirms that *smc3-D1189H* is responsible for the drug resistance. The D1189 residue is highly conserved evolutionarily, as the analogous position in all *SMC3* family members is either an aspartic acid or a glutamic acid residue (Figure 2D).

Cohesion around the centromere is essential to enable sister kinetochores to reform bipolar attachments after their transient detachment from spindle microtubules. Therefore we assumed that *smc3-D1189H eco1*Δ *wpl1*Δ cells acquired benomyl resistance because cohesion was restored at centromere-proximal regions. To test this idea, we began by comparing the level of cohesion at the centromere-linked *TRP1* locus in wild-type, *eco1*Δ *wpl1*Δ, and our reconstructed *smc3-D1189H eco1*Δ *wpl1*Δ strain. The *smc3-D1189H eco1*Δ *wpl1*Δ cells had restored cohesion relative to *eco1*Δ *wpl1*Δ but not fully restored to wild-type levels (Figure 3A). This level of cohesion is sufficient to explain the benomyl resistance, as it is similar to the cohesion level and benomyl resistance seen in a *wpl1*Δ strain (compare Figures 1C and 3A; Guacci and Koshland, 2012). We then tested whether the cohesion restored by *smc3-D1189H* as measured via the GFP-spot assay is functional, segregation-competent cohesion using our nocodazole-arrest release segregation assay (Figure 1B). Because *smc3-D1189H eco1*Δ *wpl1*Δ and *wpl1*Δ cells have similar levels of cohesion, we compared their ability to promote segregation. After release from nocodazole arrest, *smc3-D1189H eco1*Δ *wpl1*Δ segregated sister chromatids properly in 80% of cells, much better than the random 50% segregation observed in *eco1*Δ *wpl1*Δ cells and nearly as well as *wpl1*Δ or wild-type cells (Figure 3B). Therefore the cohesion restored by *smc3-D1189H* is segregation competent. Moreover, *smc3-D1189H* eliminates the sub-1C peak found in *eco1*Δ *wpl1*Δ cells, suggesting global restoration of cohesion (Figure 3B). Because *smc3-D1189H*

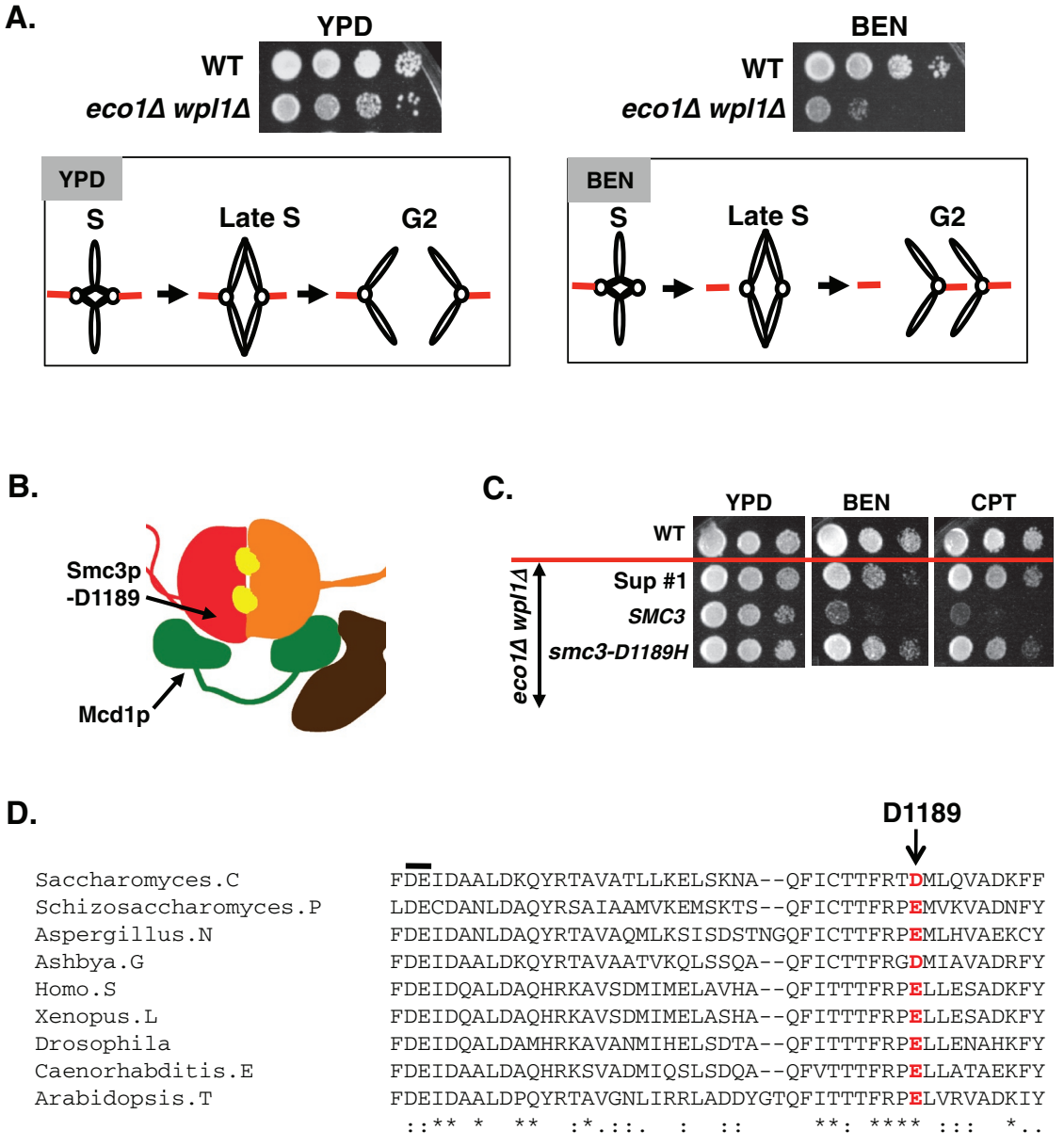

FIGURE 2: Genetic screen identifies the *smc3-D1189H* mutation as a suppressor of *eco1*Δ *wpl1*Δ strain sensitivity to benomyl and camptothecin. (A) Rationale for screen. Haploid WT (VG3349-1B) and *eco1*Δ *wpl1*Δ (VG3503-4A) were grown to saturation at 23°C, plated at 10-fold serial dilution on YPD alone or containing 12.5 µg/ml BEN, and then incubated at 23°C for 3 d. Left, *eco1*Δ *wpl1*Δ cell viability on YPD and schematic showing sister segregation via early S-phase attachments despite failure to establish cohesion. Right, *eco1*Δ *wpl1*Δ cell inviability on BEN and schematic showing benomyl-induced loss of S-phase spindle attachments and consequent missegregation and inviability. (B) Cartoon showing localization of the D1189 residue in the *SMC3* head domain. (C) Cross drug resistance of the *smc3-D1189H* suppressor. Haploid WT (3460-2A) and three *eco1*Δ *wpl1*Δ background strains, parent *SMC3* (VG3502-1A), D1189H suppressor 1 (Sup #1), and rebuilt *smc3-D1189H* (VG3547-3B), were grown and plated as described in A onto YPD alone or containing 12.5 µg/ml BEN or 10 µg/ml CPT and incubated for 3 d at 23°C. Strains below the red line are *eco1*Δ *wpl1*Δ background. (D) Schematic showing evolutionary conservation of budding yeast *smc3-D1189* residue (red letter). The black line above the sequence shows the conserved DE residues of the Smc3p Walker B box.

restores cohesion to *eco1*Δ *wpl1*Δ cells, we term it a cohesion activator mutation.

To further characterize the partial restoration of cohesion in *smc3-D1189H eco1*Δ *wpl1*Δ cells, we examined cohesion at *TRP1* as cells progressed through the cell cycle as compared with wild-type and *eco1*Δ *wpl1*Δ cells. Cells were released from G1 into media containing nocodazole to induce mid–M phase arrest. Cell aliquots were fixed in G1 and at 20-min intervals after G1 release to assess cohesion and DNA content. As expected for wild-type cells, separated sister chromatids were rarely observed, indicative of robust cohesion (Figure 3C). The *eco1*Δ *wpl1*Δ cells exhibited separated sister chromatids (two GFP spots) beginning in S phase, consistent with a previously reported establishment defect (Guacci and Koshland, 2012). Fewer *smc3-D1189H eco1*Δ *wp1*Δ cells exhibited two GFP spots than *eco1*Δ *wpl1*Δ cells, but the kinetics of cohesion loss was similar, as it also begins during S phase. These results indicate that

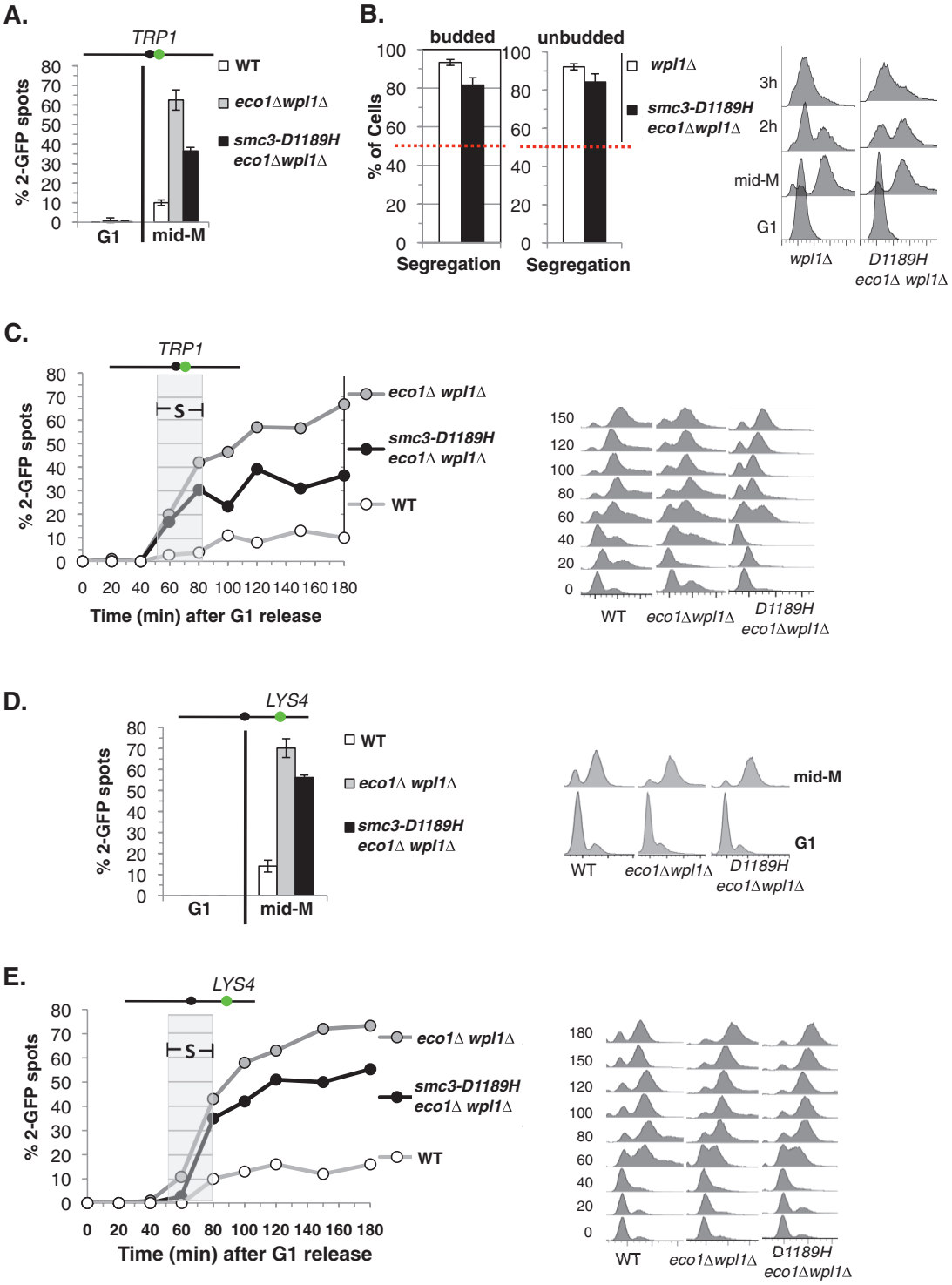

FIGURE 3: *smc3-D1189H* partially restores sister chromatid cohesion in *eco1*Δ *wpl1*Δ cells. (A) Cohesion loss at a *CEN*-proximal *TRP1* locus. Haploid WT (VG3460-2A), *eco1*Δ *wpl1*Δ (VG3502-1C), and *smc3-D1189H eco1*Δ *wpl1*Δ (VG3547-3B) were arrested in mid–M phase as described in Figure 1C. The percentage of cells with two GFP signals (sister separation) is plotted. The lack of G1 cells with two GFP spots demonstrates absence of preexisting aneuploidy. Data are from four independent experiments; 100–300 cells were scored for each data point in each experiment. (B) Assay for segregation-competent cohesion. Haploid *smc3-D1189H eco1*Δ *wpl1*Δ (VG3549-7A) and *wpl1*Δ (VG3513-1B) cells were treated as depicted in Figure 1B and then assayed for chromosome segregation after release from mid–M arrest. Proper segregation of chromosome IV sister chromatids in large-budded cells 2 h after release (left) and in unbudded cells 3 h after release (middle) and DNA content (right). Random segregation will be 50% and is marked by a dotted red line. Data were generated simultaneously with strains in Figure 1, C–E, in two independent experiments in which 100–300 cells were scored for each data point. (C) Kinetics of cohesion loss at a *CEN*-proximal *TRP1* locus. Strains in A released from G1 and arrested in mid–M phase as described in Figure 1C. The percentage of cells with two GFP

smc3-D1189H promotes cohesion establishment in the *eco1*Δ *wp1*Δ background, but the residual cohesion defect is due to incomplete restoration of establishment rather than a defect in cohesion maintenance. We next examined cohesion at the *CEN*-distal (*LYS4*) locus in these strain backgrounds. The *smc3-D1189H* allele also partially suppresses the cohesion establishment defect of *eco1*Δ *wpl1*Δ (Figure 3, D and E). Note that the suppression was less robust than at the *CEN*-distal locus compared with the *CEN*-proximal locus.

smc3-D1189H cohesin responds to regulators as well as wild-type cohesin

The partial restoration of cohesion by *smc3-D1189H* in the *eco1*Δ *wpl1*Δ background could reflect the inability of *smc3-D1189H* to fully compensate for cohesion defects caused by the absence of Eco1p and Wpl1p. Alternatively, it could be due to a cohesion defect caused by *smc3-D1189H* itself. To test whether the *smc3-D1189H* mutation has inherent defects in cohesion and cohesin function, we generated an otherwise wild-type yeast strain bearing *smc3-D1189H* as the sole *SMC3* allele (*Materials and Methods*). Wild-type and *smc3-D1189H* cells were assayed for drug sensitivity and showed similar strong resistance to both benomyl and camptothecin (Figure 4A). We next assayed cohesion at *CEN*-proximal (*TRP1*) and *CEN*-distal (*LYS4*) loci, as well as cohesin binding to CARs via chromatin immunoprecipitation (ChIP). Wild-type and *smc3-D1189H* cells were released from G1 and arrested in mid–M phase (*Materials and Methods*). Few mid–M phase cells had two GFP spots in either wild-type or *smc3-D1189H* cells, indicating that both strains had robust cohesion (Figure 4B). Analysis of the chromosomal binding of cohesin subunits shows that they colocalize, making the analysis of any one a surrogate marker for cohesin binding (Glynn *et al.*, 2004; Lengronne *et al.*, 2004; Heidinger-Pauli *et al.*, 2010). We used antibodies against Mcd1p (αMcd1p) as a marker to detect cohesin binding to chromosomes. ChIP showed no difference in Mcd1p binding at the *CEN*-proximal *CARC1* or the *CEN*-distal *CARL1* in these two strains (Figure 4C). Thus *smc3-D1189H* appears fully competent to promote cohesion and to respond normally to cohesion regulation by both Eco1p and Wpl1p. Finally, the Scc2p loader complex is required for cohesion and viability in wild-type cells (Ciosk *et al.*, 2000). *Smc3-D1189H* cells also require Scc2p for both viability and cohesion (Supplemental Figure S4). These results show that *smc3-D1189H* cohesin functions as well as wild-type (WT) cohesin when normal cohesin regulation is present. Therefore the partial suppression of the cohesion defect of *eco1*Δ *wpl1*Δ cells by *smc3-D1189H* is not due to an inherent cohesion defect associated with *smc3-D1189H*. Instead, it indicates that *smc3-D1189H* restores only a subset of the Eco1p and/or Wpl1p activities.

smc3-D1189H does not suppress the cohesion defect of a *wpl1*Δ

The residual cohesion defect in *smc3-D1189H eco1*Δ *wpl1*Δ (35% sister chromatid separation at *TRP1*) is very similar to that of a *wpl1*Δ mutant alone (compare Figures 1C and 3A; Guacci and Koshland, 2012). This similarity could reflect that *smc3-D1189H* robustly suppresses the *eco1*Δ without affecting the cohesion defect caused by a *wpl1*Δ. Alternatively, it could reflect complete suppression of *wpl1*Δ, but only partial suppression of the *eco1*Δ. We first addressed whether *smc3-D1189H* suppresses a *wpl1*Δ. One signature of a *wpl1*Δ is a reduction in cohesin bound at CARs as compared with WT cells (Rowland *et al.*, 2009; Sutani *et al.*, 2009). In contrast, an *eco1* mutant does not reduce cohesin binding at CARs (Noble *et al.*, 2006). Therefore, if *smc3-D1189H* in *eco1*Δ *wpl1*Δ suppressed the loss of Wpl1p, we would expect it to increase cohesin binding to WT levels. We examined whether *smc3-D1189H* affects cohesin binding to chromosomes in the *eco1*Δ *wpl1*Δ background. Cells were released from G1 and then rearrested in mid–M phase (*Materials and Methods*). Mid–M phase cells were processed to assess cohesin binding to chromosomes using both chromosome spreads and ChIP.

We first used chromosome spreads to qualitatively assess cohesin binding to chromosomes. We detected robust Mcd1p staining on chromosomal DNA in wild-type, *eco1*Δ *wpl1*Δ, and *smc3-D1189H eco1*Δ *wpl1*Δ cells, indicative of broad cohesin binding (Figure 5A). We then used ChIP to perform a quantitative analysis of cohesin binding at two CARs—one in the pericentric region of chromosome III (*CARC1*) and one at a *CEN*-distal locus (*CARL1*). Mcd1p binding at either CAR site was reduced by twofold to threefold in the *eco1*Δ *wpl1*Δ cells compared with wild type (Figure 5B). This degree of reduction was previously reported for *wpl1*Δ and *eco1*Δ *wpl1*Δ cells (Sutani *et al.*, 2009). The *smc3-D1189H eco1*Δ *wpl1*Δ cells exhibit the same reduced cohesin binding as the parent *eco1*Δ *wpl1*Δ cells (Figure 5B). Thus *smc3-D1189H* did not suppress the cohesin-loading defect characteristic of a *wpl1*Δ. Moreover, this result indicates that the improved sister chromatid cohesion engendered by *smc3-D1189H* in *eco1*Δ *wpl1*Δ cells occurs via a mechanism distinct from increasing cohesin localization to CARs.

To assess specifically whether *smc3-D1189H* affects the *wpl1*Δ cohesion defect, we analyzed its effect when Eco1p is present. For this purpose, we constructed an *smc3-D1189H wpl1*Δ strain and compared its phenotype to that of a *wpl1*Δ strain. The *smc3-D1189H* is unable to suppress the slight camptothecin sensitivity of a *wpl1*Δ (Figure 4A). In addition, the *smc3-D1189H wpl1*Δ strain exhibited a very similar cohesion defect as the *wpl1*Δ strain (Figure 5C). These results suggest that *smc3-D1189H* partially restores cohesion in *eco1*Δ *wpl1*Δ cells by recapitulating Eco1p activity rather than compensating for the loss of Wpl1p.

smc3-D1189H suppresses the requirement for Eco1p-mediated Smc3p K112 K113 acetylation in cohesion generation

Eco1p acetylates sites on cohesin subunits and cohesin regulators (Ivanov *et al.*, 2002; Rolef Ben-Shahar *et al.*, 2008; Unal *et al.*, 2008; Zhang *et al.*, 2008). Smc3p is acetylated at both K112 and K113, but

spots is plotted (left) along with DNA content (right). Gray box shows S phase. Between 100 and 300 were cells scored for each data point. (D, E) Cohesion loss at a *CEN*-distal *LYS4* locus. Haploid wild-type (VG3349-1B), *eco1*Δ *wpl1*Δ (VG3503-4A), and *smc3-D1189H eco1*Δ *wpl1*Δ (VG3549-7A) were arrested in mid–M phase arrest as described in Figure 1C. (D) Cohesion loss at mid–M phase arrest. The percentage of cells with two GFP spots is plotted (left) along with DNA content (right). Data were derived from two independent experiments, and 100–300 cells were scored for each data point. (E) Time course to assess kinetics of cohesion loss. The percentage of cells with two GFP spots is plotted (left) along with DNA content (right). Gray box shows S phase. Between 100 and 300 were cells scored for each data point. The green dot above the graph shows the position of LacO arrays relative to the centromere.

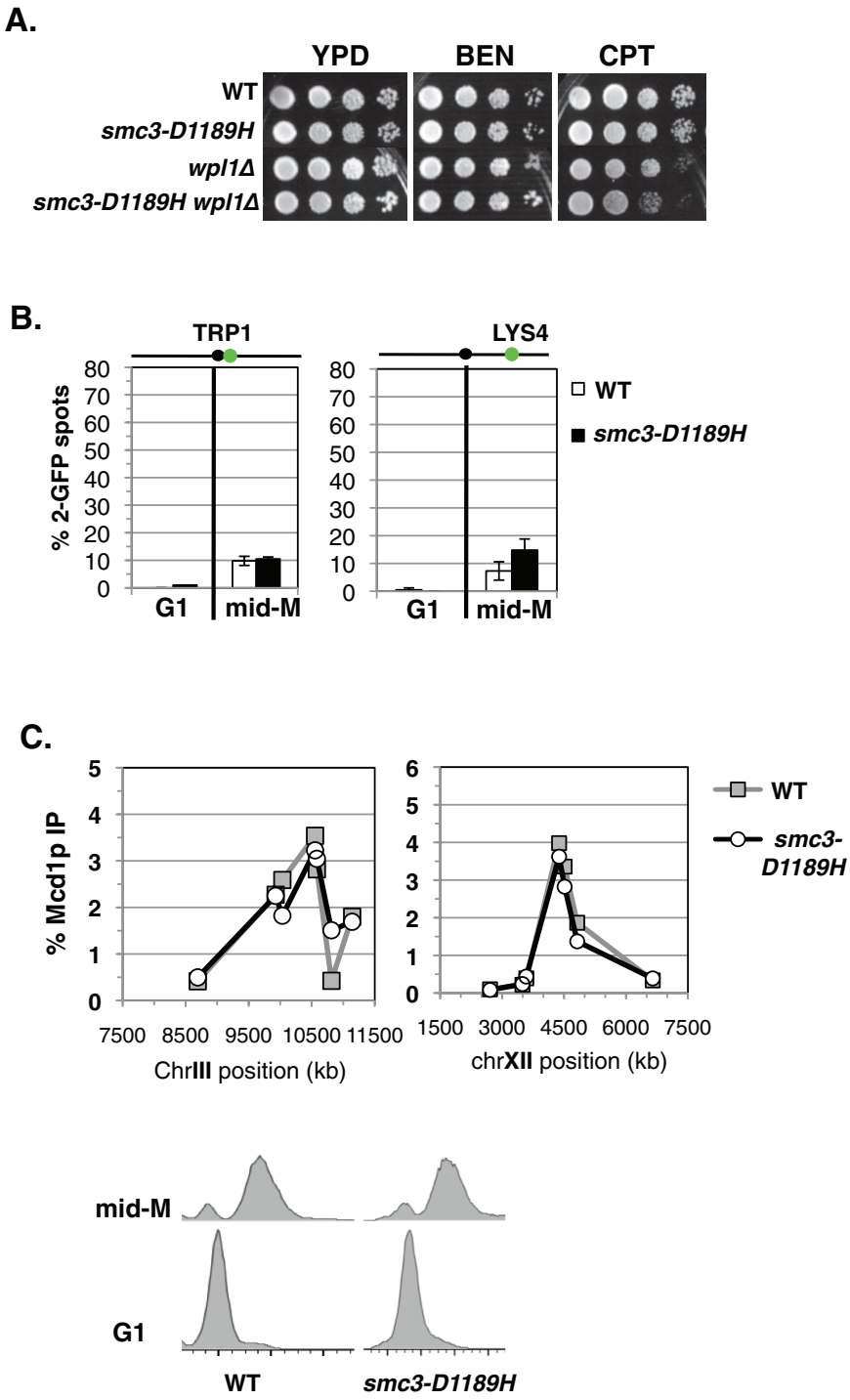

FIGURE 4: *smc3-D1189H* cohesin is fully functional in a WT background. (A) Assessing the drug sensitivity of *smc3-D1189H* cells. Haploid WT (VG3599-9C), *smc3-D1189H* (VG3600-13C), *wpl1*Δ (VG3604-4C), and *smc3-D1189H wpl1*Δ (VG3605-5D) were grown and plated onto YPD alone or containing BEN (12.5 μg/ml) or CPT (15 μg/ml) as described in Figure 2A and then incubated at 23°C for 3 d for YPD and CPT and 4 d for BEN. (B) Cohesion loss in mid–M phase cells. WT and *smc3-D1189H* cells were released from G1 and arrested in mid–M phase as described in Figure 1C. Left, cohesion loss at *CEN*-proximal *TRP1* locus in haploid WT (VG3599-9C) and *smc3-D1189H* (VG3600-13C) cells. Right, cohesion loss at *CEN*-distal *LYS4* locus in haploid WT (VG3557-2A) and *smc3-D1189H* (VG3558-2D) strains. Cohesion loss is the percentage of cells with two GFP spots. Data were derived from two independent experiments. Between 100 and 300 cells were scored for each data point in each experiment. (C) ChIP of Mcd1p in mid–M phase–arrested cells. Haploid WT (VG3599-9C) and *smc3-D1189H* (VG3600-13C) mid–M phase–arrested cells from B were subjected to ChIP using αMcd1p antibodies (top) and DNA content determined (bottom). Mcd1p binding was assessed by quantitative PCR. Data are presented as percentage of total DNA assayed using the same primer pairs at each site. Left, chromosome III pericentric *CARC1*. Seven primer pairs used to assay Mcd1p binding at loci spanning an ~2.6-kb region including *CARC1* of chromosome III. Right, chromosome XII *CEN*-distal *CARL1*. Seven primer pairs used to assay Mcd1p binding at loci spanning an ~4.5-kb region including *CARL1* of chromosome XII. WT (gray line, gray squares) and *smc3-D1189H* (black line, open circles).

K113 had been shown to be critical for cohesion (Unal *et al.*, 2008; Zhang *et al.*, 2008). The function and identity of other sites remain largely untested. Therefore it was possible that *smc3-D1189H* suppressed the *eco1*Δ *wpl1*Δ cohesion defect by providing the function of all the Eco1p substrates or of only a subset of them.

To distinguish between these possibilities, we first tested whether *smc3-D1189H* suppressed inviability and major cohesion defects associated with the failure to acetylate Smc3p K112 and K113 (Unal *et al.*, 2008; Zhang *et al.*, 2008). To assess bypass of the smc3-*K112R, K113R* acetyl-null (*smc3-RR*) inviability, we used an *SMC3* shuffle strain in which the endogenous *SMC3* is deleted but cells are kept viable by the presence of plasmid pEU42 (*SMC3 URA3 CEN*). We integrated a second "test *SMC3* allele"—wild-type *SMC3*, *smc3-D1189H*, the *K112R, K113R* acetyl-null (*smc3-RR*), or a chimeric *smc3-RR-D1189H* allele—into the shuffle strain at the *LEU2* locus. These test alleles were assayed for ability to support viability as the sole *SMC3* source by growth on media containing 5-fluoroorotic acid (FOA; *Materials and Methods*). FOA selectively kills *URA3* cells, thereby selecting for cells that had lost plasmid pEU42. As expected, all strains grew well on URA– medium because of the presence of WT *SMC3* on pEU42 (Figure 6A). On FOA medium, cells with WT *SMC3* and *smc3-D1189H* test alleles grew well, whereas the *smc3-RR* allele could not support viability. Cells bearing the chimeric *smc3-RR-D1189H* allele grew as well as on FOA medium as WT and *smc3-D1189H* cells, demonstrating that the *smc3-D1189H* mutation suppresses the inviability of the *RR* mutation (Figure 6A). We then compared the drug sensitivity of cells bearing only the WT *SMC3, smc3-D1189H*, or chimeric *smc3-RR-D1189H* test alleles as the sole *SMC3*. All strains showed equal resistance to both benomyl and camptothecin, suggesting that chimeric allele efficiently generated cohesion (Figure 6B).

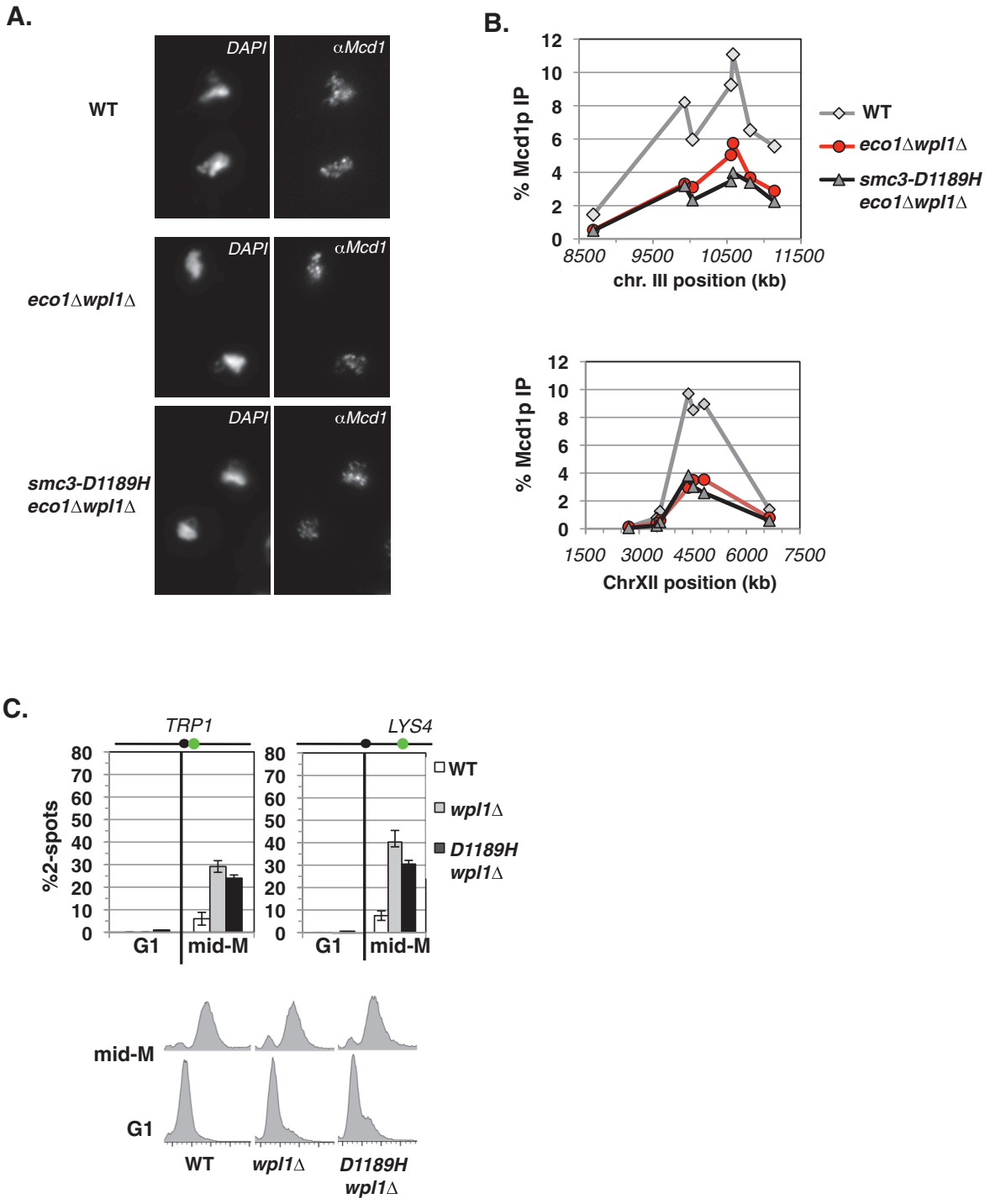

FIGURE 5: *Smc3-D1189H* fails to suppress the characteristic *wpl1*Δ defects of reduced cohesin binding and partial cohesion loss. (A–C) Haploid wild-type (WT; VG3349-1B), *eco1*Δ *wpl1*Δ (VG3503-4A), and *smc3-D1189H eco1*Δ *wpl1*Δ (VG3549-7A) cells were arrested in mid–M phase as described in Figure 1C. (A) Chromosome spreads of mid–M phase cells. WT (top), *eco1*Δ *wpl1*Δ (middle), and *smc3-D1189H eco1*Δ *wpl1*Δ (bottom). Cells were processed to detect chromosomal DNA (4′,6-diamidino-2-phenylindole) and cohesin using αMcd1p antibodies. (B) ChIP of Mcd1p in mid–M phase cells. Cells were fixed and processed for ChIP using αMcd1p antibodies. WT (gray line, gray diamonds), *eco1*Δ *wpl1*Δ (red line, red circles), and *smc3-D1189H eco1*Δ *wpl1*Δ (black line, gray triangles). Mcd1p binding was assessed as described in Figure 4C. Top, chromosome III pericentric *CARC1*. Bottom, chromosome XII *CEN*-distal *CARL*. (C) Effect of *smc3-D1189H* on cohesion loss in a *wpl1*Δ background. Haploid WT, *wpl1*Δ, and *smc3-D1189H wpl1*Δ cells were arrested in mid–M phase as described in Figure 1C. Left, cohesion loss at *CEN*-proximal *TRP1* locus assayed in haploid WT (VG3460-2A), *wpl1*Δ (VG3604-4C), and *smc3-D1189H wpl1*Δ (VG3605-5D) strains. Right, cohesion loss at *CEN*-distal *LYS4* locus assessed in haploid WT (VG3349-1B), *wpl1*Δ (VG3626-2E), and *smc3-D1189H wpl1*Δ (VG3627-3C) strains. Bottom, DNA content. The percentage of cells with two GFP signals (sister separation) is plotted. Data were derived from two independent experiments; 100–300 cells were scored for each data point in each experiment.

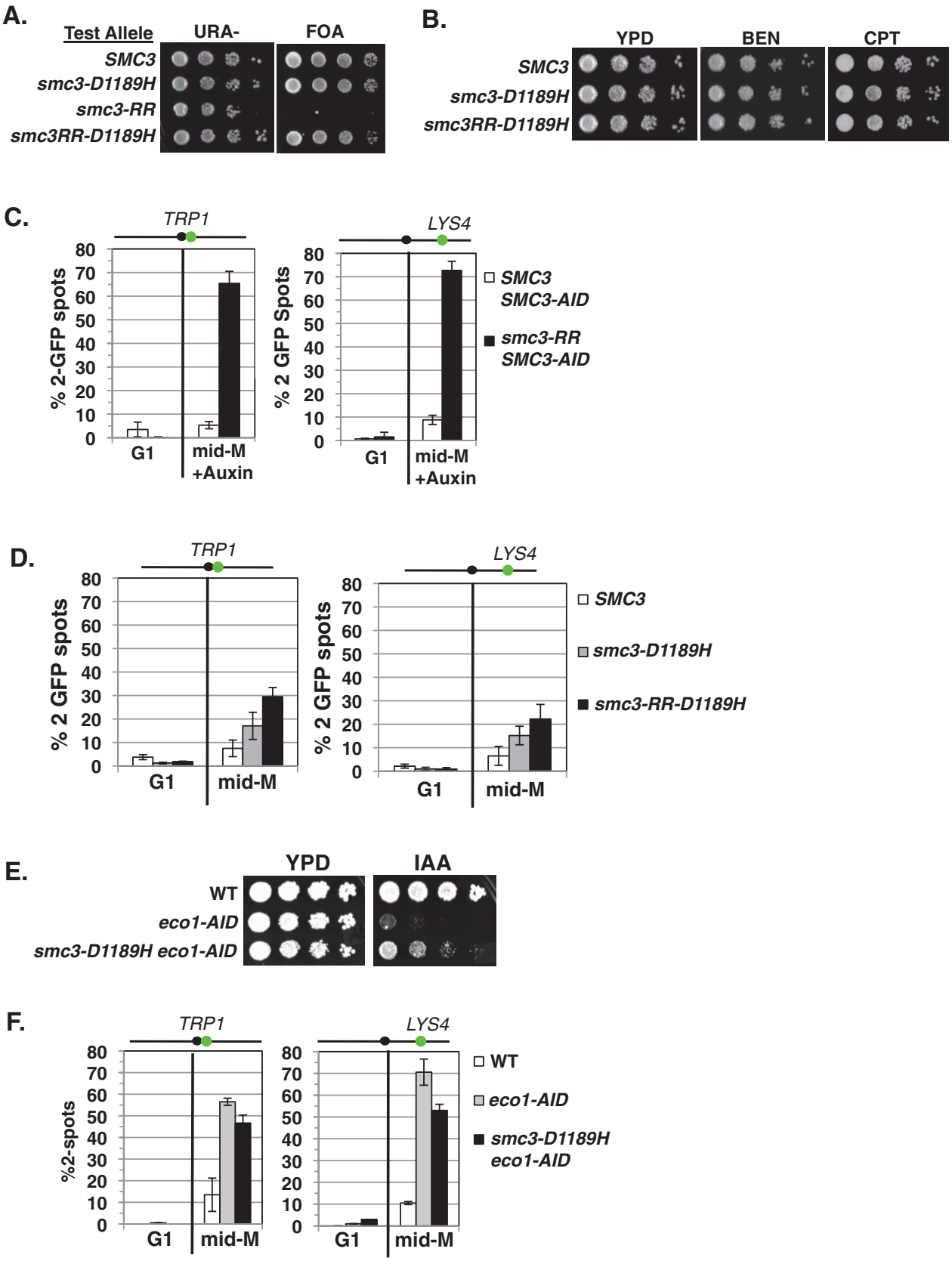

FIGURE 6: *smc3-D1189H* robustly suppresses the cohesion defect of the *smc3-K112R, K113R* (*RR*) mutation. (A) Plasmid shuffle to assess viability of the chimeric *smc3-RR-D1189H* allele. Haploid shuffle strain VG3464-16C bearing plasmid pEU42 (*SMC3 CEN URA3*) and a second *SMC3* "test allele," *SMC3*, *smc3-D1189H*, *smc3-RR*, or chimeric *smc3RR-D1189H*, was grown and plated as described in Figure 2A onto URA–dropout or FOA-containing media. Plates were

To test the suppression of the *smc3-RR* cohesion defect by *smc3-D1189H*, we compared cohesion at *CEN*-proximal and *CEN*-distal loci in cells expressing only chimeric *smc3-RR-D1189H* allele with cells expressing only the *smc3-RR* allele. Making this comparison was complicated by the fact that the *smc3-RR* allele cannot support viability (Unal *et al.*, 2008; Zhang *et al.*, 2008). Consequently, the *smc3-RR* allele was assayed in a strain bearing an *smc3* temperature-sensitive allele at nonpermissive temperature and shown to have a major cohesion defect (Unal *et al.*, 2008; Zhang *et al.*, 2008). However, we wanted to assess the *smc3-RR* allele at the low temperature (23°C) used for our previous assays. Therefore we constructed a parent strain bearing a conditional *SMC3-AID* allele, which enables the SMC3-AIDp to be rapidly degraded at 23°C upon auxin addition, rendering cells inviable and severely defective for cohesion (Supplemental Figure S5, A–C). We integrated a second *SMC3* allele, either wild-type *SMC3* or *smc3-RR*, into the *SMC3-AID*–bearing strain. As expected, the *SMC3* allele suppressed the *SMC3-AID* inviability on auxin, whereas the *smc3-RR* failed to do so (Supplemental Figure S5C). We next assessed cohesion at *CEN*-proximal and *CEN*-distal loci in cells released from G1 and arrested in mid–M phase under conditions in which SMC3-AIDp was depleted over this entire cell-cycle window (Supplemental Figures S2B and S5D). The *SMC3* allele enabled robust cohesion, whereas the *smc3-RR* cells were severely compromised for cohesion, as ~70% of cells had two GFP spots (Figure 6C), a value similar to that for strains bearing only *SMC3-AID* as the sole *SMC3* (Supplemental Figure S5B). We then examined cohesion at mid–M phase in strains in which the sole *SMC3* allele is wild-type *SMC3*, *smc3-D1189H*, or the chimeric *smc3-RR-D1189H* allele (Supplemental Figure S5E). Only 20–30% of cells in the chimeric *smc3-RR-D1189H* strain exhibited two GFP spots, a dramatic improvement over the cohesion defect of the *smc3-RR* strain and similar to that seen in either WT *SMC3* or *smc3-D1189H* cells (Figure 6D). These results indicate that the *smc3-D1189H* mutation strongly suppresses the cohesion defect generated by blocking K112, K113 acetylation.

Evidence that Eco1-dependent acetylation of sites other than Smc3-K112, K113 are required for efficient cohesion establishment

We next addressed whether *smc3-D1189H* could suppress loss of all Eco1p acetylation targets in cells as well as it suppressed the *smc3-K112, K113* acetyl null. Because *eco1*Δ cells are not viable, we used strains bearing a conditional *ECO1-AID* allele and either wild-type *SMC3* or *smc3-D1189H* as the sole *SMC3* alleles in cells. As expected, wild-type haploids grew on yeast extract/peptone/dextrose (YPD) medium either alone or containing auxin (Figure 6E). Auxin-containing medium prevented growth of *ECO1-AID* cells, but a low-level of viability was detected when the *smc3-D1189H* allele was present, indicating at best a weak suppression of the essential *ECO1* function (Figure 6E).

We then examined cohesion at *CEN*-proximal and *CEN*-distal loci in these three strains after auxin-mediated ECO1-AIDp depletion from G1 through arrest in mid–M phase (Supplemental Figures S2B and S5F). As expected, the wild-type cells had robust cohesion (10% two GFP spots), whereas the *ECO1-AID* strain had a severe cohesion defect (60–70% two GFP spots; Figure 6F). The *smc3-D1189H ECO1-AID* strain also showed a strong cohesion defect, with only modest improvement in cohesion at *CEN*-proximal and *CEN*-distal loci, respectively. Thus the chimeric *smc3-RR-D1189H* allele in a WT background generated cohesion more efficiently than the *smc3-D1189H* allele did in an *ECO1-AID* background: 15 and 30% better at *TRP1* and at *LYS4*, respectively (compare Figure 6, D and F). Therefore, whereas the *smc3-RR* and *ECO1-AID* alone have a similar ~70% cohesion defect, *smc3-D1189H* suppresses the *smc3-RR* cohesion defect much better than that of an Eco1-AIDp depletion. These results suggest that the *D1189H* mutation effectively provides the K112, K113 acetylation function but that other Eco1p acetylation targets are necessary for efficient cohesion generation.

smc3-D1189H activates cohesion by a Wpl1p-independent mechanism

Previous work showed that a *wpl1*Δ suppresses the *smc3-RR* allele lethality (Rolef Ben-Shahar *et al.*, 2008). This result raised the prospect that in the chimeric *smc3-RR-D1189H* allele, the *D1189H* mutation merely blocked the anticohesion function of Wpl1p. If true, then a *wpl1*Δ *smc3-RR* strain should be phenotypically identical to the chimeric *smc3-RR-D1189H* strain. Therefore we compared wild-type and *smc3-RR wpl1*Δ strains for viability, drug sensitivity, and cohesion generation. We first used a *wpl1*Δ *SMC3* shuffle strain to assess *smc3-RR wpl1*Δ viability and drug sensitivity compared with *SMC3 wpl1*Δ. As previously reported, the *wpl1*Δ suppresses

incubated 3 d at 23°C. (B) Assessment of drug sensitivity. Haploid *SMC3* (MB45-1A), *smc3-D1189H* (MB46-1A), or chimeric *smc3-RR-D1189H* (MB47-1A) strains grown and plated as described in Figure 2A onto YPD, BEN, and CPT and incubated at 30°C for 2 d. (C). Cohesion loss of in *smc3-RR* cells. Haploids bearing *SMC3-AID* and a second *SMC3* allele, either WT or *smc3-RR*, were depleted for *SMC3-AID* from G1 through mid–M phase arrest. Left, cohesion loss at *CEN*-proximal *TRP1* locus assessed in haploid *SMC3 SMC3-AID* (MB84-1A) and *smc3-RR SMC3-AID* (MB83-1A) strains. Right, cohesion loss at *CEN*-distal *LYS4* locus assessed in haploid *SMC3 SMC3-AID* (MB81-1A) and *smc3-RR SMC3-AID* (MB79-1A) strains. The percentage of cells with two GFP spots (sister separation) is plotted. (D) Cohesion loss of *smc3-RR-D1189H* in mid–M phase–arrested cells. Haploid *SMC3, smc3-D1189H* and chimeric *smc3-RR-D1189H* were arrested in mid–M phase as described in Figure 1B. Left, cohesion loss at *CEN*-proximal *TRP1* locus assessed in haploid wild-type (*SMC3*; MB65-1A), *smc3-D1189H* (MB66-1A), or chimeric *smc3-RR-D1189H* (MB67-1A) strain. Right, cohesion loss at *CEN*-distal *LYS4* locus assessed in haploid strains from B. The percentage of cells with two GFP spots (sister separation) is plotted. (E, F) Assessing *smc3-D1189H* ability to suppress Eco1p depletion. (E) Viability after Eco1p depletion. Haploid WT (VG3620-4C), *ECO1-AID* (VG3662-1D), and *smc3-D1189H ECO1-AID* (VG3663-2E) were grown and plated as described in Figure 2A onto YPD alone or containing auxin (750 μM) and then incubated at 23°C for 2 d. (F) Cohesion loss after auxin-mediated Eco1p depletion from G1 cells through mid–M phase arrest. Left, cohesion loss at *CEN*-proximal *TRP1* locus assayed in haploid strains WT (VG3460-2A), *ECO1-AID2* (VG3659-1A) and *smc3-D1189H ECO1-AID2* (VG3663-2E) strains. Right, cohesion loss at *CEN*-distal *LYS4* locus assessed in haploid WT (VG3620-4C), *ECO1-AID2* (VG3646-1A) and *smc3-D1189H ECO1-AID2* (VG3650-1E) strains. The percentage of cells with two GFP signals (sister separation) is plotted. (C, D, F) Data were derived from two independent experiments; 100–300 cells were scored for each data point in each experiment.

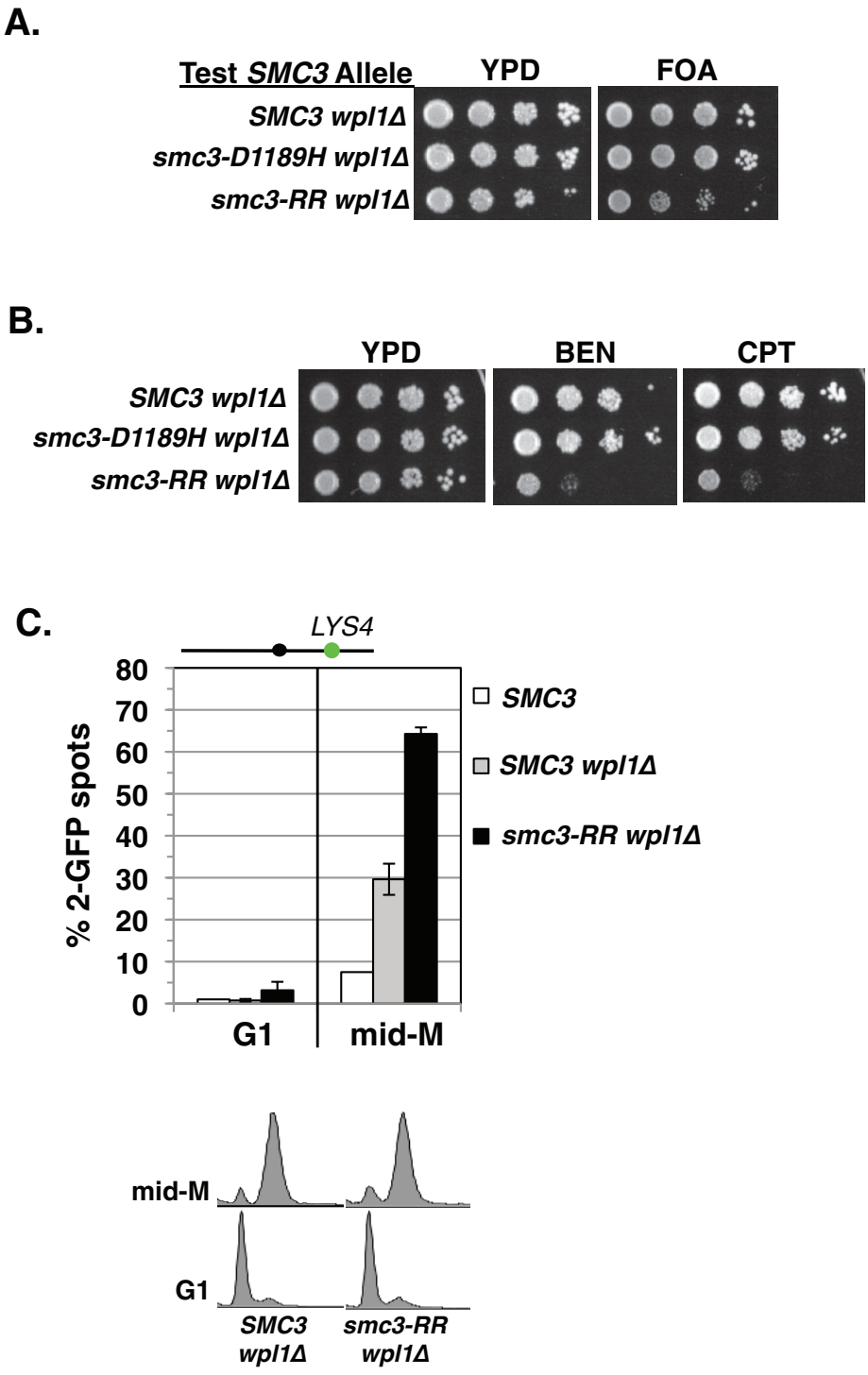

FIGURE 7: A *wpl1*Δ suppresses the inviability of *smc3-RR*–bearing cells but not the cohesion defect. (A) Plasmid shuffle to assess viability of *smc3-RR wpl1*Δ cells. Haploid *wpl1*Δ *SMC3* shuffle strain (VG3578-1A) bearing pEU42 (*SMC3 CEN URA3*) and a second integrated test *SMC3* allele—WT (*SMC3 wpl1*Δ), *smc3-D1189H* (*smc3-D1189H wpl1*Δ), or *smc3-RR* (*smc3-RR wpl1*Δ)—were grown and plated as described in Figure 2A onto URA–dropout or FOA-containing media. Plates were incubated 2 d at 30°C. (B) Assessment of *smc3-RR wpl1*Δ strain drug sensitivity. Haploid *SMC3 wpl1*Δ (MB48-1A), *smc3-D1189H wpl1*Δ (VG3627-3C), and *smc3-RR wpl1*Δ (MB50-1A) strains were grown and plated as described in Figure 2A onto YPD alone or containing BEN (10 μg/ml) or CPT (10 μg/ml) and incubated at 23°C for 3 d for YPD and 4 d for BEN and CPT plates. (C) Cohesion loss at *CEN*-proximal locus *LYS4*. Haploid wild-type (WT; VG3627-3C), *wpl1*Δ (*SMC3 wpl1*Δ; MB48-1A), and *smc3-RR wpl1*Δ (MB50-1A) strains arrested in mid–M phase as described in Figure 1B. Cells were scored for cohesion loss (top) and DNA content (bottom). Data are derived from two independent experiments; 100–300 cells were scored for each data point in each experiment.

smc3-RR allele inviability (Figure 7A). However, unlike the chimeric *smc3-RR-D1189H* strain, the *smc3-RR wpl1*Δ strain is highly sensitive to both benomyl and camptothecin, suggestive of a major cohesion defect (Figure 7B). Indeed, when we examined cohesion in mid–M phase–arrested cells, *smc3-RR wpl1*Δ cells had as dramatic a defect (~70% two GFP spots) as the *smc3-RR* cells (Figure 7C). Thus *wpl1*Δ failed to suppress the cohesion defect engendered by *smc3-RR*, whereas *smc3-D1189H* suppressed it very well. These results demonstrate that *smc3-D1189H* bypasses the *smc3-RR* defect in cohesion by a mechanism distinct from antagonizing Wpl1p. Moreover, it demonstrates that a Wpl1p-independent step is required for sister chromatid cohesion.

DISCUSSION

The prevailing Wpl1p-centric model posits that the Eco1p acetyltransferase promotes cohesion establishment simply by antagonizing Wpl1p-mediated inhibition (Rowland *et al.*, 2009; Sutani *et al.*, 2009; Chan *et al.*, 2012). Contrary to this model, we previously showed that *eco1*Δ *wpl1*Δ cells have little or no cohesion, based on in vivo monitoring of specific chromosomal GFP-tagged loci (Guacci and Koshland, 2012). We suggested that Eco1p promotes cohesion establishment by a Wpl1p-independent mechanism. Here we provide additional in vivo metrics to support the absence of cohesion in *eco1*Δ *wpl*Δ cells. First, we used a nocodazole arrest–release assay, which uses proper chromosome segregation as a sensitive readout for the presence of residual cohesion on a chromosome. We find that *eco1*Δ *wpl1*Δ cells, like cohesin subunit mutants, lack segregation competent cohesion (this study; Guacci and Koshland, 2012).

The lack of cohesion in *eco1*Δ *wpl1*Δ is also supported by published cytological observations from other laboratories. Before anaphase, yeast cells have a short mitotic spindle overlaid by a short bilobed barrel of centromeres and a single DNA mass (Pearson *et al.*, 2004; Yeh *et al.*, 2008). However, cohesion-defective yeast precociously elongate their spindle to generate two widely spaced centromere clusters and two separated DNA masses (Yeh *et al.*, 2008). Both an *eco1* mutant and an *eco1*Δ *wpl1*Δ double mutant exhibit the same phenotype of widely spaced centromere clusters and two separated DNA masses (Skibbens *et al.*, 1999; Chan *et al.*, 2012), indicative of an equivalent global failure in spindle-restraining cohesion.

We also identified *smc3-D1189H* as a mutation that significantly restores cohesion

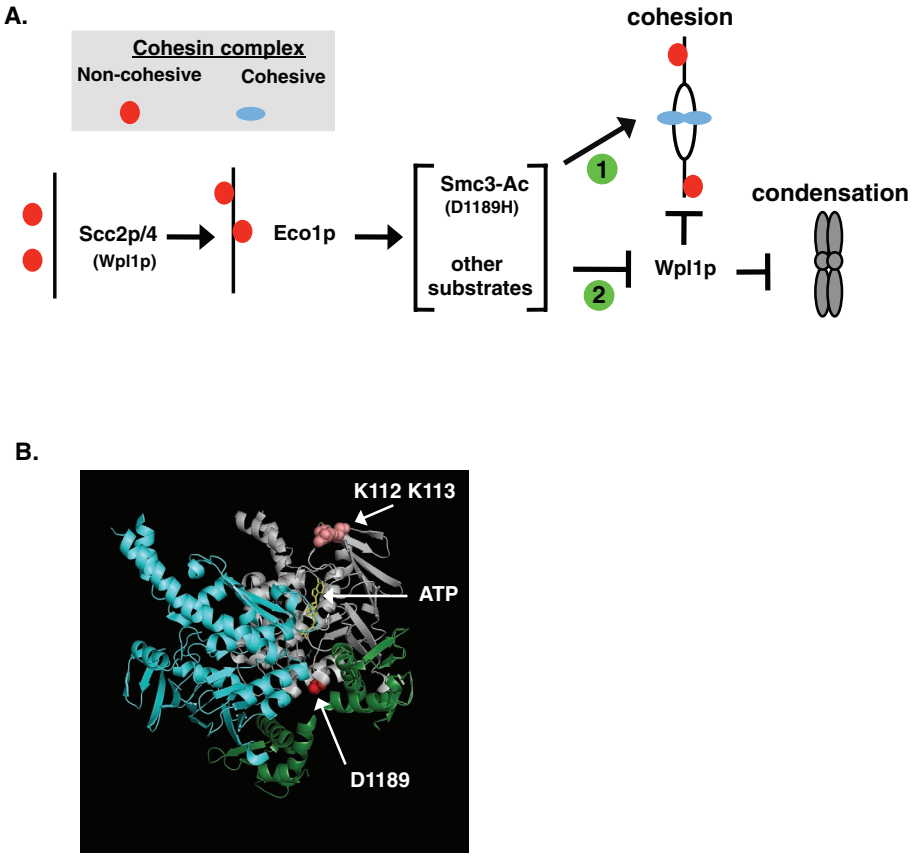

FIGURE 8: Regulatory and structural model for Eco1p-mediated regulation of cohesin. (A) Model of cohesin regulation. Eco1p-mediated acetylation of Smc3p and other targets play a Wpl1p-independent role to promote cohesion establishment (arrow 1) and overcome Wpl1p inhibition of condensation and cohesion (T-bar 2). Cohesin in the noncohesive form (red circles) and a cohesive form (blue ovals) are shown. (B) *smc3-D1189* modeled on Smc1p crystal structure. Shown are the head domains of Smc3p (gray) and Smc1p (blue) bound as a dimer to Mcd1p N-terminus and C-terminus (green). Indicated by arrows are the D1189 residue (red) at the bottom of Smc3p, the ATP molecule in the Smc3p Walker A/B box (yellow), and the Smc3-K112, K113 residues (salmon colored).

in *eco1Δ wpl1Δ* cells as measured by both the GFP-spot assay and presence of segregation-competent cohesion. Taken together, these independent in vivo measures of cohesion strongly corroborate our previous conclusion that *wpl1Δ* poorly, if at all, suppresses the cohesion defect of *eco1Δ*. Moreover, because both *eco1Δ wpl1Δ* and *wpl1Δ smc3-RR* cells exhibit major defects in cohesion and are very sensitive to both benomyl and camptothecin, we propose that these dual drug sensitivities represent signatures of cohesion-defective cells. Thus Eco1p promotes cohesion establishment by a Wpl1p- independent mechanism that was missed by previous studies.

The characterization of the *smc3-D1189H* cohesion activator mutation provides important clues about this unrecognized Wpl1p-independent mechanism for cohesion generation. *Smc3-D1189H* robustly suppresses the cohesion defect of an acetylation-null *smc3-K112R, K113R*, whereas a *wpl1Δ* fails to suppress the *K112R, K113R* cohesion defect. This stark difference between *smc3-D1189H* and *wpl1Δ* further validates that Eco1p acetylation of Smc3p K112, K113 promotes cohesion by Wpl1p-independent mechanism (Figure 8A, arrow 1). The K112, K113, and D1189 and residues are in the Smc3p head domain, suggesting a common mechanism for modulating cohesin. No crystal structure of the Smc3p head is available, and so we used the structure of the related Smc1p head bound to the Mcd1p C-terminus as a surrogate for Smc3p head binding to the Mcd1p N-terminus (Haering *et al.*, 2004). Although D1189 does not appear to be in close proximity to K112, K113 residues, it is in a region that could alter interactions with Mcd1p and or affect Smc3p ATPase function (Figure 8B). The latter is intriguing, as we previously proposed a connection between K112, K113 acetylation and Smc3 ATPase function based on genetic interactions between mutations in K112, K113 and mutations of Walker B residues required for hydrolysis residues (Heidinger-Pauli *et al.*, 2010).

The *smc3-D1189H* allele suppresses the cohesion defect of *smc3-K112R, K113R* much better than the defect when *ECO1* function is lost. This difference suggests that Eco1p acetylates other targets besides Smc3p K113 to promote cohesion (Figure 8A, arrow 1). The view is supported by the observations that Smc3 K113 and K112, K113 acetyl mimics (glutamine or asparagine residues) only partially suppress the cohesion defect of reduced Eco1p activity (Unal *et al.*, 2008). Eco1p acetylates itself, Mcd1p (Scc1p), Scc3p, and the cohesin regulator, Pds5p (Ivanov *et al.*, 2002). Of these, only the Mcd1p substrate has been examined, and its acetylation has no role during S-phase cohesion but instead promotes DNA damage repair cohesion (Heidinger-Pauli *et al.*, 2009). Further studies of other Eco1p targets are needed to elucidate how cohesion is regulated.

We find that although a *wpl1Δ* does restore viability to *smc3-RR* or *eco1Δ* cells, it fails to restore cohesion. Similarly, the *smc3-K112R, K113Q* acetyl-mimic allele restores viability without restoring cohesion (Guacci and Koshland, 2012). We previously showed that the *smc3-K112R, K113Q* allele, like a *wpl1Δ* in *eco1Δ* background, restores condensation (Guacci and Koshland, 2012). This led to the idea that Smc3p acetylation overcomes Wpl1p inhibition of an essential cohesin function, likely condensation (Figure 8A, T-bar 2; Guacci and Koshland, 2012). *smc3-D1189H* restores viability to *smc3-RR* cells without restoring cohesion, which fits with the idea that *D1189H* mimics acetylation to promote condensation. The limited ability of *smc3-D1189H* to suppress the inviability of *ECO1-AID* depletion suggests that other Eco1p targets besides *Smc3-K112, K113*, possibly Wpl1p itself, also contribute to condensation (Figure 8A, T-bar 2).

The fact that cohesion is defective in both *eco1Δ wpl1Δ* and *smc3-K112R,K113R* cells provides insights into the mechanism of cohesion (this study; Guacci and Koshland, 2012). Cohesin binding to chromosomes is as stable in *smc3-K112R, K113R* cells as in wild-type cells but is more stable in *eco1Δ wpl1Δ* cells (Rowland *et al.*, 2009; Chan *et al.*, 2012). Therefore the failure to acetylate Smc3p does not compromise cohesin binding to chromatin but likely mediates a subsequent step necessary for cohesion. Consistent with this conclusion, *Smc3-D1189H* does not alter cohesin binding levels on chromosomes in *eco1Δ wpl1Δ* cells despite partially restoring cohesion. We suggest that Smc3p acetylation/smc3-D1189Hp promote

cohesion establishment by converting the stably bound cohesin to a tethering form (Figure 8A, arrow 1). Recent studies support the idea that a second step distinct from stable cohesin binding to DNA is required for cohesion maintenance (Eng *et al.*, 2014; Tong and Skibbens, 2014).

The nature of this second step remains to be determined. A new study on the related Smc condensin complex provided evidence for a two-step mode of DNA binding (Piazza *et al.*, 2014). One can envision cohesin having two sites of different DNA binding that are differentially regulated—one used for cohesin binding and the second for sister tethering. Alternatively, models from studies of the Smc-like Rad50 or bacterial Smc complexes suggest that Smc complexes oligomerize, potentially by changes in the coiled-coil domain conformation (Hopfner *et al.*, 2002; Woo *et al.*, 2009; Bürmann *et al.*, 2013). Finally, a recent study of bacterial Smc complexes revealed that its kleisin (Mcd1p) subunit binds the coiled coils as well as the Smc heads (Bürmann *et al.*, 2013). This structure provides a potential mechanism by which Smc3p acetylation and/or ATPase could alter kleisin (Mcd1p) binding to the coiled-coil domain. Whether this alters Mcd1p-Smc head binding, Smc3p head conformation, or longer-range cohesin structure remains an open question. Testing these ideas will require in vitro biochemical assays for which the *D1189H* mutation provides a powerful new reagent.

Do other organisms require additional Eco1p acetylation sites and the Wpl1p-independent function of Eco1p for cohesion establishment? One functional study in *Schizosaccharomyces pombe* suggested that additional sites besides the Smc3p K112, K113 equivalent lysines (Psm3-K105R, K106R) are needed for centromere-proximal cohesion (Feytout *et al.*, 2011). In contrast, the existence of a Wpl1p-independent function for Eco1p might appear less likely, as the cohesion defect associated with reduced Eco1p activity in *S. pombe* and vertebrate cells appears to be significantly suppressed by reduction in *WPL1* activity (Gandhi *et al.*, 2006; Feytout *et al.*, 2011; Vaur *et al.*, 2012). However, closer scrutiny suggests that this conclusion may be premature. In vertebrates, WAPL (Wpl1p orthologue) removes ~95% of chromosomally bound cohesin from prophase to metaphase (Losada *et al.*, 1998; Sumara *et al.*, 2000; Gandhi *et al.*, 2006; Kueng *et al.*, 2006). The remaining 5% of cohesin is sufficient to tether sisters, although cohesion is less robust and sisters become more separated and resolved. Small interfering RNA (siRNA) depletion of the *ECO1* orthologue ESCO2 generates metaphase chromosomes with significantly defective cohesion, whereas codepletion of WAPL and ESCO2 was reported to reduce this cohesion defect (Gandhi *et al.*, 2006). However, these experiments compared distinct chromosomal states—prophase (siRNA both WAPL and ESCO2) versus metaphase (siRNA of just ESCO2)—that have greatly different levels of cohesin bound. The extra bound cohesin on the prophase-like chromosomes could obscure a significant cohesion defect. Therefore the existence of a WAPL-independent function of Eco1p remains an open question in vertebrates.

In *S. pombe*, unlike budding yeast and vertebrates, acetylation of Smc3p at K112, K113 equivalents (Psm3-K105R,K106R) is not essential (Feytout *et al.*, 2011). Similarly, the cohesin regulator Pds5p is not essential in *S. pombe* but is essential in budding yeast and metazoans (Hartman *et al.*, 2000; Tanaka *et al.*, 2001; Dorsett, 2005; Vaur *et al.*, 2012). This difference remains despite the fact that physical interactions between Pds5p and Eco1p have been demonstrated in both yeasts (Tanaka *et al.*, 2001; Noble *et al.*, 2006). Perhaps cohesin regulation in *S. pombe* has been simplified during evolution so as to contain natural variants that function analogous to budding yeast *smc3-D1189H*, bypassing the need for Eco1p-mediated activation of cohesion establishment. Indeed, our initial characterization of other cohesion activators in *eco1Δ wpl1Δ* cells suggests multiple targets for potential natural variants.

Although additional studies will be necessary to tease out these potential differences of cohesin regulation between species, the underlying mechanism of its cohesion activity is undoubtedly conserved. Further studies of the *D1189H* mutation and other *eco1Δ wpl1Δ* cohesion activators will provide powerful new reagents to elucidate cohesin regulation and function.

MATERIALS AND METHODS

Yeast strains and media

Yeast strains used in this study are A364A background, and their genotypes are listed in Supplemental Table S1. SC minimal and YPD media were prepared as described (Guacci *et al.*, 1997). Benomyl (a gift from Dupont, Wilmington, DE) and camptothecin (Sigma-Aldrich, St. Louis, MO) plates used to assess drug sensitivity were prepared as previously described (Guacci and Koshland, 2012). Preparation of media containing auxin (Sigma-Aldrich) for depletion of AID tagged proteins was as previously described (Eng *et al.*, 2014).

Dilution plating assays

Cells were grown to saturation in YPD medium at 23°C (or 30°C when listed) and then plated in 10-fold serial dilutions. Cells were incubated on plates at relevant temperatures or containing drugs as described. For plasmid shuffle assays, cells were grown to saturation in YPD medium to allow loss of plasmid pEU42 (*SMC3 CEN URA3*) and then plated in 10-fold serial dilutions.

G1 arrest and release into mid–M phase arrest

G1 arrest. Asynchronous cultures of cells were grown to mid log phase at 23°C in YPD medium, and then αFactor (Sigma-Aldrich) was added to 10^{-8} M. Cells were incubated for 3 h to induce arrest in G1 phase. This incubation time was increased to 3.5 h for all strains in any experiment in which an *eco1Δ wpl1Δ* background strain was used. For depletion of AID tagged proteins, auxin was added (500 μM final) and cells incubated an additional 1 h in αFactor-containing medium.

Release from G1 into mid–M phase arrest. G1 arrested cells were washed three times in YPD containing 0.1 mg/ml Pronase E (Sigma-Aldrich) and once in YPD and then resuspended in YPD containing nocodazole (Sigma-Aldrich) at 15 μg/ml final. Cells were incubated at 23°C for 3 h to arrest in mid–M phase. For depletion of AID-tagged proteins, auxin was added (500 μM final) in all wash media and in resuspension media containing nocodazole to ensure depletion at all times.

Nocodazole arrest–release assay for chromosome IV segregation

Cells were arrested in G1 phase and then released and rearrested in mid–M phase using nocodazole as described. Cells were washed three times with YPD and then resuspended in YPD containing αFactor (10^{-8} M) and incubated 4 h at 23°C

Scoring segregation in large-budded (telophase) cells. Large-budded cells after nocodazole arrest–release were scored for proper chromosome IV sister segregation. Only cells with two GFP signals were scored. Cells were scored as exhibiting segregation when there was one GFP signal in each daughter bud. The percentage of chromosome IV sister chromatids scored as having segregated was calculated as (large-budded cells with segregated sisters/total number of large-budded cells) × 100.

Scoring segregation in unbudded (G1 phase) cells. After cell division, segregation generates two cells with one GFP spot each, whereas missegregation generates one cell with two GFP spots and one cell with no GFP spots. Therefore the percentage of unbudded cells showing segregation was calculated as (unbudded cells with one GFP signal/total number of unbudded cells) × 100.

Genetic screen of *eco1Δ wpl1Δ* cells for cohesion activator suppressors

Our results indicate that *eco1Δ wpl1Δ* cells have little or no cohesion and are sensitive to benomyl (BEN) and camptothecin (CPT; Guacci and Koshland, 2012). BEN destabilizes microtubules and so induces detachment of early S-phase kinetochore–microtubule attachments essential for cohesin-independent segregation (Figure 2A). CPT inhibits topoisomerase I, which induces single-strand nicks that can become double-strand DNA breaks (DSBs) during replication in S phase. Because cohesin/cohesion play a role in DSB repair (Ström *et al*., 2004; Unal *et al*., 2004), CPT lethality is likely due to a combination of reduced repair of DSBs and DNA-damage checkpoint–induced cell-cycle delays, increasing the likelihood of loss kinetochore–microtubule attachments formed in S phase.

We wanted to identify mutations that restore cohesion to *eco1Δ wpl1Δ* cells. We reasoned that suppressors that restore cohesion in *eco1Δ wpl1Δ* cells will be resistant to both drugs, and so we conducted a genetic screen on this basis. To set the parameter for the screen, we assayed haploid *eco1Δ wpl1Δ* cells for the BEN and CPT concentrations that induce complete lethality when 10^6 cells are plated (Supplemental Figure S3A). For the screen, haploid *eco1Δ wpl1Δ* cells were dilution streaked on YPD plates and grown at 23°C to enable formation of colonies from single cells (Supplemental Figure S3B). A small amount of one single colony was inoculated into YPD liquid medium and grown to saturation at 23°C. Aliquots containing ~2×10^7 cells were plated onto YPD containing either BEN or CPT at 12.5–15 μg/ml and then incubated 4–5 d at 23°C. Twenty-four different single colonies were subjected to this regimen to generate a pool of suppressors with independent origins. A few drug-resistant colonies (suppressors) arose on each plate. Suppressor clones were retested for resistance to the same drug and for cross-resistance—that is, BEN-resistant clones tested for CPT resistance and vice versa. Suppressors that exhibited cross drug-resistance were subjected to whole-genome sequencing using TruSeq DNA Sample v2 Kit (Illumina, San Diego, CA).

Monitoring cohesion using LacO-GFP assay

Cohesion was monitored using the LacO-LacI system, in which cells contained a GFP-LacI fusion and tandem LacO repeats integrated at one chromosomal locus, which recruits the GFP-LacI (Straight *et al*., 1996). *CEN*-distal cohesion was monitored by integrating LacO repeats at *LYS4*, located 470 kb from *CEN4*. *CEN*-proximal cohesion is monitored by integrating LacO at *TRP1*, located 10 kb from *CEN4*. Cells were fixed and processed to allow the number of GFP signals in each cell to be scored and the percentage of cells with two GFP spots determined as previously described (Guacci and Koshland, 2012). Bulk chromosomal DNA for imaging was visualized as previously described (Guacci and Koshland, 2012).

Plasmid constructs

Site-directed mutagenesis using the QuikChange Site Directed Mutagenesis Kit (Agilent Technologies, Santa Clara, CA) was used to generate the *smc3-D1189H* allele on *URA3* or *LEU2* integration plasmid pVG441 D1189H (*smc3-D1189H URA3*) or pVG419 D1189H (*smc3-D1189H LEU2*), respectively. The *smc3-D1189H* mutation was confirmed by sequencing the entire open reading frame (ORF), as well as the promoter region, to ensure that it was the only change.

Strain construction

SMC3 shuffle strain construction. Haploids containing plasmid pEU42 (*SMC3 URA3 CEN*) had their endogenous *SMC3* gene deleted and replaced by the HPH cassette (encodes resistance to hygromycin B [Roche Biologicals, Indianapolis, IN]) using standard PCR-mediated, homology-based recombination.

Assessment of SMC3 test alleles by integration at the LEU2 locus. A second *SMC3* "test allele" was cloned onto an integrating vector (pVG419; *SMC3 LEU2*) and linearized within *LEU2* by *Bst*EII digestion. Linearized plasmid pVG419 bearing WT or *smc3* mutant alleles was transformed into shuffle strains to integrate them at the *LEU2* locus, and LEU+ transformants were selected. These "test alleles" were assayed for their ability to support viability as the sole *SMC3* source as follows. LEU+ clones were grown to saturation in YPD medium at 23°C to allow loss of plasmid pEU42 and then plated in 10-fold serial dilutions on medium containing FOA (US Biologicals, Salem, MA). FOA selectively kills *URA3* cells, thereby selecting for loss of pEU42, which allows assessment of test allele ability to support viability as the sole *SMC3* in cells. As a control, cells were also plated on either YPD or URA–medium. This shuffle strategy was used to create WT, *wpl1Δ*, and *eco1Δ wpl1Δ* cells with *smc3-D1189H* alleles integrated at the *LEU2* locus as the sole *SMC3*.

Insertion of SMC3 alleles at the endogenous locus. Two different strategies were used. One used *SMC3* shuffle strains described earlier for one step-gene replacement. A linear DNA fragment containing the desired *SMC3* ORF allele, *SMC3* promoter, and 3′ untranslated region were transformed into shuffle strains, plated on YPD, and grown overnight. Plates were replica plated to FOA, and FOA-resistant clones were selected and tested for sensitivity to hygromycin B, which occurs when *smc3Δ::HPH* is replaced by the transformed linear *SMC3* allele. Transplacement alleles were confirmed by PCR screening and PCR sequencing.

The second strategy to replace the *SMC3* allele with *smc3-D1189H* allele in haploid *eco1Δ wpl1Δ* cells or to replace *SMC3* with *SMC3-AID* in WT cells bearing *TIR1* was as follows. Plasmid pVG441 D1189H (*smc3-D1189H URA3*) or pVG465 (*SMC3-AID URA3*) was linearized within the *SMC3* ORF by *Psh*AI digestion. Linearized pVG441 or pVG465 was transformed into haploid *eco1Δ wpl1Δ* strains (VG3502-1A and VG3503-4C) or a wild-type *TIR1* strain (VG3620-4C), respectively. URA+ colonies contain the *SMC3 URA3* plasmid integrated at the *SMC3* locus to create tandem *SMC3* genes. URA+ transformants were replica plated onto YPD and then dilution streaked on FOA to excise the *URA3* marker and thereby select for loss of one *SMC3* allele. PCR-mediated sequencing was used to identify clones containing only the *smc3-D1189H* or *SMC3-AID* allele.

Strains containing *AID*-tagged proteins

Details of the auxin-mediated destruction of AID-tagged proteins in yeast was previously described (Eng *et al*., 2014). Briefly, the *TIR1* E3-ubiquiting ligase placed under control of the GPD promoter and marked by *Candida albicans TRP1* replaced the *TRP1* gene on chromosome IV. *ECO1* and *SCC2* were C-terminally tagged with *3V5-AID2* sequences by standard PCR techniques and transformed into yeast strains bearing *TIR1* to generate *ECO1-AID* or *SCC2-AID* allele, respectively. For *SMC3-AID*, a *Bgl*II site was inserted after Smc3p amino acid residue N607 and then the *3V5-AID1* cassette

inserted on a *Bam*HI/*Bgl*II fragment via standard cloning techniques. We replaced *SMC3* with *SMC3-AID* at the endogenous locus as described. PCR screening and auxin-mediated sensitivity were used to identify clones containing *AID*-tagged genes.

Chromosome spreads

Chromosome spreads were performed as previously described, except primary that antibody was diluted in 5% bovine serum albumin, 0.2% milk, 1× phosphate-buffered saline, and 0.2% Triton X-100 (Hartman *et al*., 2000). Mcd1p was detected using rabbit anti-Mcd1p antibodies (Rb#555; αMcd1p) at a 1:10,000 dilution.

Chromatin immunoprecipitation

ChIP was performed as previously described (Wahba *et al*., 2013; Eng *et al*., 2014).

Microscopy

Images were acquired with a Zeiss Axioplan2 microscope (100× objective, numerical aperture, 1.40) equipped with a Quantix charge-coupled device camera (Photometrics).

Flow cytometry analysis

Flow cytometry analysis was performed as previously described (Eng *et al*., 2014).

ACKNOWLEDGMENTS

We thank Anjali Zimmer, Gamze Çamdere, Thomas Eng, Lorenzo Constantino, Liam Holt, Brett Robison, Rebecca Lamothe, and Elçin Ünal for critical reading of the manuscript. We thank Thomas Eng, Gamze Çamdere, and Jessica Poon for technical support and all other members of the Koshland lab for support and helpful comments. This work was funded by National Institutes of Health Grant R01GM092813.

REFERENCES

Blat Y, Kleckner N (1999). Cohesins bind to preferential sites along yeast chromosome III, with differential regulation along arms versus the centric region. Cell 98, 249–259.

Bürmann F, Shin H-C, Basquin J, Soh Y-M, Giménez-Oya V, Kim Y-G, Oh B-H, Gruber S (2013). An asymmetric SMC-kleisin bridge in prokaryotic condensin. Nat Struct Mol Biol 20, 371–379.

Chan K-L, Roig MB, Hu B, Beckouet F, Metson J, Nasmyth K (2012). Cohesin's DNA exit gate is distinct from its entrance gate and is regulated by acetylation. Cell 150, 961–974.

Ciosk R, Shirayama M, Shevchenko A, Tanaka T, Toth A, Nasmyth K (2000). Cohesin's binding to chromosomes depends on a separate complex consisting of Scc2 and Scc4 proteins. Mol Cell 5, 243–254.

Dorsett D (2005). Effects of sister chromatid cohesion proteins on cut gene expression during wing development in Drosophila. Development 132, 4743–4753.

Eng T, Guacci V, Koshland D (2014). ROCC, a conserved region in cohesin's Mcd1 subunit, is essential for the proper regulation of the maintenance of cohesion and establishment of condensation. Mol Biol Cell 25, 2351–2364.

Feytout A, Vaur S, Genier S, Vazquez S, Javerzat J-P (2011). Psm3 acetylation on conserved lysine residues is dispensable for viability in fission yeast but contributes to Eso1-mediated sister chromatid cohesion by antagonizing Wpl1. Mol Cell Biol 31, 1771–1786.

Gandhi R, Gillespie PJ, Hirano T (2006). Human Wapl is a cohesin-binding protein that promotes sister-chromatid resolution in mitotic prophase. Curr Biol 16, 2406–2417.

Glynn EF, Megee PC, Yu H-G, Mistrot C, Unal E, Koshland DE, DeRisi JL, Gerton JL (2004). Genome-wide mapping of the cohesin complex in the yeast Saccharomyces cerevisiae. PLoS Biol 2, E259.

Guacci V, Hogan E, Koshland D (1994). Chromosome condensation and sister chromatid pairing in budding yeast. J Cell Biol 125, 517–530.

Guacci V, Koshland D (2012). Cohesin-independent segregation of sister chromatids in budding yeast. Mol Biol Cell 23, 729–739.

Guacci V, Koshland D, Strunnikov A (1997). A direct link between sister chromatid cohesion and chromosome condensation revealed through the analysis of MCD1 in S. cerevisiae. Cell 91, 47–57.

Haering CH, Schoffnegger D, Nishino T, Helmhart W, Nasmyth K, Löwe J (2004). Structure and stability of cohesin's Smc1-kleisin interaction. Mol Cell 15, 951–964.

Hartman T, Stead K, Koshland D, Guacci V (2000). Pds5p is an essential chromosomal protein required for both sister chromatid cohesion and condensation in Saccharomyces cerevisiae. J Cell Biol 151, 613–626.

Heidinger-Pauli JM, Onn I, Koshland D (2010). Genetic evidence that the acetylation of the Smc3p subunit of cohesin modulates its ATP-bound state to promote cohesion establishment in Saccharomyces cerevisiae. Genetics 185, 1249–1256.

Heidinger-Pauli JM, Unal E, Koshland D (2009). Distinct targets of the Eco1 acetyltransferase modulate cohesion in S phase and in response to DNA damage. Mol Cell 34, 311–321.

Hopfner K-P, Craig L, Moncalian G, Zinkel RA, Usui T, Owen BAL, Karcher A, Henderson B, Bodmer JL, McMurray CT, *et al*. (2002). The Rad50 zinc-hook is a structure joining Mre11 complexes in DNA recombination and repair. Nature 418, 562–566.

Ivanov D, Schleiffer A, Eisenhaber F, Mechtler K, Haering CH, Nasmyth K (2002). Eco1 is a novel acetyltransferase that can acetylate proteins involved in cohesion. Curr Biol 12, 323–328.

Kim J-S, Krasieva TB, LaMorte V, Taylor AMR, Yokomori K (2002). Specific recruitment of human cohesin to laser-induced DNA damage. J Biol Chem 277, 45149–45153.

Kueng S, Hegemann B, Peters BH, Lipp JJ, Schleiffer A, Mechtler K, Peters J-M (2006). Wapl controls the dynamic association of cohesin with chromatin. Cell 127, 955–967.

Laloraya S, Guacci V, Koshland D (2000). Chromosomal addresses of the cohesin component Mcd1p. J Cell Biol 151, 1047–1056.

Lengronne A, Katou Y, Mori S, Yokobayashi S, Kelly GP, Itoh T, Watanabe Y, Shirahige K, Uhlmann F (2004). Cohesin relocation from sites of chromosomal loading to places of convergent transcription. Nature 430, 573–578.

Lopez-Serra L, Lengronne A, Borges V, Kelly G (2013). Budding yeast Wapl controls sister chromatid cohesion maintenance and chromosome condensation. Curr Biol 23, 64–69.

Losada A, Hirano M, Hirano T (1998). Identification of Xenopus SMC protein complexes required for sister chromatid cohesion. Genes Dev 12, 1986–1997.

Megee PC, Mistrot C, Guacci V, Koshland D (1999). The centromeric sister chromatid cohesion site directs Mcd1p binding to adjacent sequences. Mol Cell 4, 445–450.

Michaelis C, Ciosk R, Nasmyth K (1997). Cohesins: chromosomal proteins that prevent premature separation of sister chromatids. Cell 91, 35–45.

Noble D, Kenna MA, Dix M, Skibbens RV, Unal E, Guacci V (2006). Intersection between the regulators of sister chromatid cohesion establishment and maintenance in budding yeast indicates a multi-step mechanism. Cell Cycle 5, 2528–2536.

Onn I, Heidinger-Pauli JM, Guacci V, Unal E, Koshland DE (2008). Sister chromatid cohesion: a simple concept with a complex reality. Annu Rev Cell Dev Biol 24, 105–129.

Pearson CG, Yeh E, Gardner M, Odde D, Salmon ED, Bloom K (2004). Stable kinetochore-microtubule attachment constrains centromere positioning in metaphase. Curr Biol 14, 1962–1967.

Piazza I, Rutkowska A, Ori A, Walczak M, Metz J, Pelechano V, Beck M, Haering CH (2014). Association of condensin with chromosomes depends on DNA binding by its HEAT-repeat subunits. Nat Struct Mol Biol 21, 560–568.

Rolef Ben-Shahar T, Heeger S, Lehane C, East P, Flynn H, Skehel M, Uhlmann F (2008). Eco1-dependent cohesin acetylation during establishment of sister chromatid cohesion. Science 321, 563–566.

Rollins RA, Korom M, Aulner N, Martens A, Dorsett D (2004). Drosophila nipped-B protein supports sister chromatid cohesion and opposes the stromalin/Scc3 cohesion factor to facilitate long-range activation of the cut gene. Mol Cell Biol 24, 3100–3111.

Rowland BD, Roig MB, Nishino T, Kurze A, Uluocak P, Mishra A, Beckouet F, Underwood P, Metson J, Imre R, *et al*. (2009). Building sister chromatid cohesion: smc3 acetylation counteracts an antiestablishment activity. Mol Cell 33, 763–774.

Skibbens RV, Corson LB, Koshland D, Hieter P (1999). Ctf7p is essential for sister chromatid cohesion and links mitotic chromosome structure to the DNA replication machinery. Genes Dev 13, 307–319.

Stead K, Aguilar C, Hartman T, Drexel M, Meluh P, Guacci V (2003). Pds5p regulates the maintenance of sister chromatid cohesion and is

sumoylated to promote the dissolution of cohesion. J Cell Biol 163, 729–741.
Straight AF, Belmont AS, Robinett CC, Murray AW (1996). GFP tagging of budding yeast chromosomes reveals that protein-protein interactions can mediate sister chromatid cohesion. Curr Biol 6, 1599–1608.
Ström L, Lindroos HB, Shirahige K, Sjögren C (2004). Postreplicative recruitment of cohesin to double-strand breaks is required for DNA repair. Mol Cell 16, 1003–1015.
Sumara I, Vorlaufer E, Gieffers C, Peters BH, Peters JM (2000). Characterization of vertebrate cohesin complexes and their regulation in prophase. J Cell Biol 151, 749–762.
Sutani T, Kawaguchi T, Kanno R, Itoh T, Shirahige K (2009). Budding yeast Wpl1(Rad61)-Pds5 complex counteracts sister chromatid cohesion-establishing reaction. Curr Biol 19, 492–497.
Tanaka K, Hao Z, Kai M, Okayama H (2001). Establishment and maintenance of sister chromatid cohesion in fission yeast by a unique mechanism. EMBO J 20, 5779–5790.
Tomonaga T, Nagao K, Kawasaki Y, Furuya K, Murakami A, Morishita J, Yuasa T, Sutani T, Kearsey SE, Uhlmann F, *et al*. (2000). Characterization of fission yeast cohesin: essential anaphase proteolysis of Rad21 phosphorylated in the S phase. Genes Dev 14, 2757–2770.
Tong K, Skibbens RV (2014). Cohesin without cohesion: a novel role for Pds5 in Saccharomyces cerevisiae. PLoS One 9, e100470.
Tóth A, Ciosk R, Uhlmann F, Galova M, Schleiffer A, Nasmyth K (1999). Yeast cohesin complex requires a conserved protein, Eco1p(Ctf7), to establish cohesion between sister chromatids during DNA replication. Genes Dev 13, 320–333.
Unal E, Arbel-Eden A, Sattler U, Shroff R, Lichten M, Haber JE, Koshland D (2004). DNA damage response pathway uses histone modification to assemble a double-strand break-specific cohesin domain. Mol Cell 16, 991–1002.
Unal E, Heidinger-Pauli JM, Kim W, Guacci V, Onn I, Gygi SP, Koshland DE (2008). A molecular determinant for the establishment of sister chromatid cohesion. Science 321, 566–569.
Vaur S, Feytout A, Vazquez S, Javerzat J-P (2012). Pds5 promotes cohesin acetylation and stable cohesin-chromosome interaction. EMBO Rep 13, 645–652.
Wahba L, Gore SK, Koshland D (2013). The homologous recombination machinery modulates the formation of RNA-DNA hybrids and associated chromosome instability. Elife 2, e00505.
Woo J-S, Lim JH, Shin HC, Suh MK, Ku B, Lee KH, Joo K, Robinson H, Lee J, Park SY, *et al*. (2009). Structural studies of a bacterial condensin complex reveal ATP-dependent disruption of intersubunit interactions. Cell 136, 85–96.
Yeh E, Haase J, Paliulis LV, Joglekar A, Bond L, Bouck D, Salmon ED, Bloom KS (2008). Pericentric chromatin is organized into an intramolecular loop in mitosis. Curr Biol 18, 81–90.
Zhang J, Shi X, Li Y, Kim BJ, Jia J, Huang Z, Yang T, Fu X, Jung SY, Wang Y, *et al*. (2008). Acetylation of Smc3 by Eco1 is required for S phase sister chromatid cohesion in both human and yeast. Mol Cell 31, 143–151.